Solution Synthesis, Conformational Analysis, and Antimicrobial Activity of Three Alamethicin F50/5 Analogs Bearing a Trifluoroacetyl Label

by **Marta De Zotti**[*a]), **Gema Ballano**[a]), **Micha Jost**[a]), **Evgeniy S. Salnikov**[b]), **Burkhard Bechinger**[b]), **Simona Oancea**[c]), **Marco Crisma**[a]), **Claudio Toniolo**[a]), and **Fernando Formaggio**[a])

[a]) ICB, Padova Unit, CNR, Department of Chemistry, University of Padova, I-35131 Padova (e-mail: marta.dezotti@unipd.it)

[b]) Membrane Biophysics and NMR, Chemistry Institute, UMR 7177, University of Strasbourg/CNRS, F-67070 Strasbourg

[c]) Department of Biochemistry and Toxycology, University 'Lucian Blaga', RO-550012 Sibiu

We prepared, by solution-phase methods, and fully characterized three analogs of the membrane-active peptaibiotic alamethicin F50/5, bearing a single trifluoroacetyl (Tfa) label at the N-terminus, at position 9 (central region) or at position 19 (C-terminus), and with the three Gln at positions 7, 18, and 19 replaced by Glu(OMe) residues. To add the Tfa label at position 9 or 19, a γ-trifluoroacetylated α,γ-diaminobutyric acid (Dab) residue was incorporated as a replacement for the original Val^{9} or Glu(OMe)^{19} amino acid. We performed a detailed conformational analysis of the three analogs (using FT-IR absorption, CD, 2D-NMR, and X-ray diffraction), which clearly showed that Tfa labeling does not introduce any dramatic backbone modification in the predominantly α-helical structure of the parent peptaibiotic. The results of an initial solid-state ^{19}F-NMR study on one of the analogs favor the conclusion that the Tfa group is a very promising reporter for the analysis of peptaibiotic–membrane interactions. Finally, we found that the antimicrobial activities of the three newly synthesized analogs depend on the position of the Tfa label in the peptide sequence.

Introduction. – In the extremely large family of the naturally occurring antimicrobial peptides (AMPs) [1–3], *peptaibiotics* [4] are members of a peculiar and promising class, as they possess the following unique features: *i*) they are active against a variety of bacteria and viruses [5][6], even drug-resistant strains [7][8]; *ii*) their α-amino acid sequences are usually quite short (between 5 and 20 amino acid residues), which is a good starting point for a potential industrial production; *iii*) nonetheless, they exhibit stable and rigid helical conformations, so that it is possible to use them as reliable scaffolds for drug delivery or other types of applications; *iv*) they are resistant to the action of proteolytic enzymes, a key feature for the development of orally administrable drugs. Moreover, the mechanism of action of peptaibiotics is of great interest, because, apparently, they do not possess a specific target, such as, for instance, an enzyme for 'conventional' antibiotics [1–3][6]. Conversely, they exploit their toxicity by perturbing the permeability of the bacterial membrane, eventually causing its leakage. This mechanism is highly promising, because it reduces the possibility for the bacteria to develop resistance. Indeed, numerous studies have been published with the aim of shedding light on the membrane interaction mechanism of peptaibiotics, making use of several different spectroscopic techniques applied to tailor-made synthetic analogs bearing suitable probes [4].

All of the properties of peptaibiotics mentioned above are due to the presence, in their sequences, of a large number of $C^{\alpha,\alpha}$-dialkyl glycines, the most common of which is α-aminoisobutyric acid (Aib), which also gives the name to this peptide family (pept*aib*iotics) [4]. Being sterically hindered, Aib can adopt almost exclusively φ,ψ angles, falling in a limited region of the *Ramachandran* plot, namely that including the helical conformation(s) [9–14]. For this reason, Aib is a strong helix inducer, but, for the same reason, its synthetic insertion in a peptide sequence is rather challenging [15–17]. Therefore, despite their great potential, single, purified peptaibiotics have been so far prepared only by specialized researchers who overcame the synthetic difficulties, which had also precluded for a long time the employment of automatic synthesizers.

The most extensively investigated peptaibiotic is alamethicin, a 19-amino acid residue-long peptide produced through non-ribosomal synthesis by the fungus *Trichoderma viride* as a mixture of numerous components, the most widely present of which is alamethicin F50/5 (**Alm**; *cf. Table 1*) [4][18–32]. Studies on how alamethicin interacts with membranes have contributed significantly to the advancement of our knowledge on the antimicrobial mechanism of peptaibiotics [33–43] and membrane pore formation in general [19].

One emerging spectroscopic technique, likely to bring an important contribution to this field is solid-state (ss) ^{19}F-NMR and, in particular, the center band-only detection of exchange (CODEX) experiment [44]. The employment of ^{19}F as the heteronucleus allows collection of reliable information on the number of molecules in the aggregates [45]. In this context, our groups have recently studied the quaternary arrangement of the self-aggregated helices of a ^{19}F-labeled alamethicin component within lipid bilayers [46]. It is then of great importance to find reliable and optimized synthetic strategies to insert ^{19}F labels, suitable for CODEX experiments, in the sequences of peptaibiotics, without affecting their overall 3D-structure.

Table 1. *Amino Acid Sequences of Alamethicin F50/5 and Its Analogs Discussed in This Article*

Name	Sequence[a])	Abbreviation
Alamethicin F50/5	Ac-Aib-Pro-Aib-Ala-Aib-Ala-Gln-Aib-Val-Aib-Gly-Leu-Aib-Pro-Val-Aib-Aib-Gln-Gln-Phol	**Alm**
[Glu(OMe)^{7,18,19}]-Alamethicin F50/5	Ac-Aib-Pro-Aib-Ala-Aib-Ala-Glu(OMe)-Aib-Val-Aib-Gly-Leu-Aib-Pro-Val-Aib-Aib-Glu(OMe)-Glu(OMe)-Phol	**Alm′** (**1**)
[(Tfa)^{0},Glu(OMe)^{7,18,19}]-Alamethicin F50/5	**Tfa**-Aib-Pro-Aib-Ala-Aib-Ala-Glu(OMe)-Aib-Val-Aib-Gly-Leu-Aib-Pro-Val-Aib-Aib-Glu(OMe)-Glu(OMe)-Phol	**N$^{\alpha}$TfaAlm′** (**2**)
[Dab(Tfa)^{9},Glu(OMe)^{7,18,19}]-Alamethicin F50/5	Ac-Aib-Pro-Aib-Ala-Aib-Ala-Glu(OMe)-Aib-**Dab(Tfa)^{9}**-Aib-Gly-Leu-Aib-Pro-Val-Aib-Aib-Glu(OMe)-Glu(OMe)-Phol	**DabTfa9Alm′** (**3**)
[Glu(OMe)^{7,18},Dab(Tfa)^{19}]-Alamethicin F50/5	Ac-Aib-Pro-Aib-Ala-Aib-Ala-Glu(OMe)-Aib-Val-Aib-Gly-Leu-Aib-Pro-Val-Aib-Aib-Glu(OMe)-**Dab(Tfa)^{19}**-Phol	**DabTfa19Alm′** (**4**)

[a]) Ac, acetyl; Phol is the 1,2-amino alcohol phenylalaninol; Dab(Tfa), γ-trifluoroacetylated α,γ-diaminobutyric acid.

Recently, the solid-phase peptide syntheses (SPPS) of selected peptaibiotics have been reported [47–56]. However, the results obtained for the longest members of this family in terms of yield and purity of the crude are still far from being satisfactory. In the present work, we exploited a solution-phase synthetic protocol to prepare three **Alm** analogs (*Table 1*), each bearing a single Tfa group *i*) at the N-terminus, *ii*) near the C-terminus (position 19), or *iii*) in the middle of the sequence (position 9). On the basis of the synthetic routes already set up for **Alm** and its Glu(OMe)[7,18,19] analog [6][18][19], hereafter termed **Alm′** (**1**), found to be as active as the parent peptaibiotic [30], we partially modified the backbone and side-chain protection strategy, thus improving the final, overall yield. The protocol for the solution-phase synthesis of these analogs is herein discussed in detail. In addition, the suitability of the Tfa probe in terms of its influence on the peptaibiotic conformation was assessed by a variety of spectroscopic techniques (FT-IR absorption, CD, 2D-NMR, and X-ray diffraction). The results of an antibacterial/antifungal investigation on the three trifluoroacetylated analogs of **Alm′** (**1**) are also presented. A preliminary account of part of this work was already reported [57].

Results and Discussion. – *Peptide Synthesis.* The challenges connected with the synthesis of peptaibiotics, due to the low reactivity (particularly at the α-amino function) of the C^{α}-tetrasubstituted α-amino acids, such as Aib [15][16], especially when two (or more) of them consecutively occur in the target sequence, and the acid lability of the extensively present Aib-Pro and Aib-Hyp ((4*R*)-4-hydroxyproline (Hyp)) bonds, are well-documented [15][16]. Nonetheless, in the past few years attempts were made
by a few research groups at preparing peptaibiotics by using the SPPS approach. However, even though short peptaibiotics and segments thereof were obtained in acceptable yield and purity [47][48], the results achieved for the long peptaibiotic alamethicin are not yet sufficiently good to exploit this methodology for a relatively large-scale synthesis.

Motivated by these findings, we planned the preparation of the three Tfa-labeled **Alm** analogs by solution-phase synthesis, in particular by taking advantage of the strategies previously described by some of us [29][30] (*solution*-phase syntheses of **Alm** and selected analogs have been already reported by other groups [58–62]). These strategies imply the use of a combination of step-by-step and segment condensation approaches (for the latter, by splitting the target sequence into segments at the level of the Aib-Pro(Hyp) bonds). *Inter alia*, this protocol offers the following advantages: *i*) the formation of the Aib-Pro(Hyp) bonds in the final synthetic steps allows one to avoid the well-established propensity of this dipeptide at the N-terminus of a sequence to cyclize to 2,5-dioxopiperazine with the concomitant loss of these two residues from the growing peptide chain, *ii*) the presence of an achiral Aib residue at the C-terminus of the peptide to be activated reduces dramatically the risk of epimerization usually inherent to the segment condensation approach, *iii*) the Aib-Pro(Hyp) bonds, if already synthetically incorporated in the peptide, would force one to avoid the use of some of the most common protecting groups such as (*tert*-butoxy)carbonyl (Boc) or *tert*-butoxy (^{t}BuO), known to be cleaved by acidic treatment. In contrast, this type of protections may be effectively employed in the step-by-step synthesis of each segment,

as envisaged in our protocol. In these strategies, however, a still existing problem is the moderate yield (30%) in the sterically hindered Aib-Pro bond-formation using the peptide oxazol-5(4*H*)-one C-component.

In this context, it is worth pointing out that, in our first syntheses of **Alm** and two analogs by use of this approach [29], we performed chiral gas-chromatographic analyses to characterize all final products and found no evidence for the potential epimerization of the penultimate Leu residue of the C-component. This finding is corroborated by our HPLC and NMR data on the present synthetic peptaibiotics which do not suggest formation of any epimer mixture.

In the present work, we maintained the same pattern of segments as described in [29][30], but we modified some of the orthogonal protections with the purpose of accommodating appropriately the different functionalities in our Tfa-labeled target sequences (*Table 1*) and improving the reaction yields. For instance, the alcohol function of the C-terminal 1,2-amino alcohol Phol (phenylalaninol) can be used without protection, because it is not nucleophilic enough to efficiently compete with peptide bond-formation under our experimental conditions. However, protecting this moiety as a benzyl (Bn) ether would increase peptide solubility in organic solvents and consequently enhance the final overall yield. Therefore, the C-terminal segment employed in the synthesis of two of the analogs discussed in this work, **N$^{\alpha}$TfaAlm′** (**2**; *Scheme 2*) and **DabTfa9Alm′** (**3**; *Table 1*), was obtained using the step-by-step procedure as outlined in *Scheme 1*. This segment corresponds to the C-terminal sequence of **Alm′** (**1**). The overall yield for the synthesis of this segment increased from

Scheme 1. *Synthetic Strategy Adopted for the* **Alm′** (**1**) *C-terminal Segment Boc-Pro-Val-(Aib)$_2$-[Glu(OMe)]$_2$-Phol*

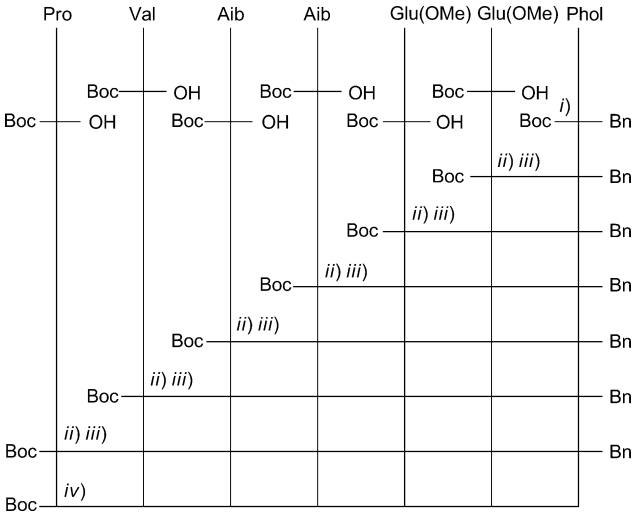

i) Boc-Phol/NaH/BnBr 1:1:1, anh. THF. *ii*) 10 equiv. of CF_3COOH (TFA), anh. CH_2Cl_2. *iii*) 1-Ethyl-3-[3-(dimethylamino)propyl]carbodiimide (EDC)/1-hydroxy-7-azabenzotriazole (HOAt), *N*-methylmorpholine (NMM; to keep pH 8). *iv*) H_2/Pd, MeOH, 4 d.

Scheme 2. *Synthesis of* **N$^{\alpha}$TfaAlm′ (2)**

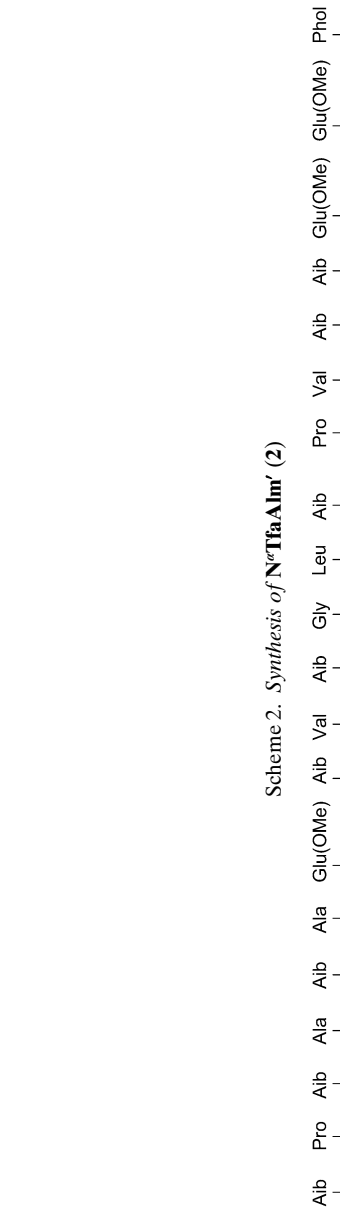

i) 10 equiv. TFA, anh. CH_2Cl_2 [30]. *ii*) TFA, anh. CH_2Cl_2 (removal of Boc from the *C*-terminal segment obtained as described in *Scheme 1*). *iii*) Segment condensation through formation of the mildly *C*-activated octapeptide oxazol-5(4*H*)-one. *iv*) EDC/HOAt, NMM (to keep pH 8). *v*) TFA, CH_2Cl_2. *vi*) H_2/Pd, MeOH. *vii*) H_2/Pd, MeOH. *viii*) EDC/HOAt, NMM (to keep pH 8).

18% (with the unprotected Phol) [29] to 24% (with the present strategy involving Phol protection).

Furthermore, we synthesized the C-terminal segment needed to obtain the **DabTfa19Alm′** (**4**) analog following either of the two synthetic pathways, namely with or without the Bn protection of the C-terminal Phol. It turned out that the protection of the Phol alcoholic moiety is indeed strongly advisable, as it allowed us to improve the yield of this C-terminal segment from 5% to more than 16%. Moreover, we found that we could exploit the *same* building block Z-Dab(Tfa)-OH (Z, (benzyloxy)carbonyl) for the synthesis of *both* target analogs **DabTfa9Alm′** (**3**; *Scheme 3*) and **DabTfa19Alm′** (**4**; *Scheme 4*), *i.e.*, in the latter case, also in the presence of Phol-Bn, making the overall schemes simpler and the related syntheses faster. Indeed, we could selectively and quantitatively remove the *N*-protecting group Z in the presence of the C-terminal Bn ether thanks to the difference between the kinetics of their removal reactions, the former requiring less than 1 h, while the latter needs several days of catalytic hydrogenation [63]. Unfortunately, no mechanistic explanation for this interesting finding was provided by the authors.

The versatile strategies employed to prepare the N-terminal (residues 1–5) and central (residues 6–13) segments are illustrated in *Schemes 2–4*. The total syntheses of the three target analogs were carried out with moderate overall yields (10–12%, more than 100 mg each) and high purities (> 95%). The protocol in [29] indicated a 6% overall yield for **Alm′** (**1**). The HPLC elution profiles (which replace the data on the TLC runs reported for all intermediate compounds) of the three fluorinated analogs of **Alm**, depicted in *Fig. 1*, highlight the purities of these final products. The analog with

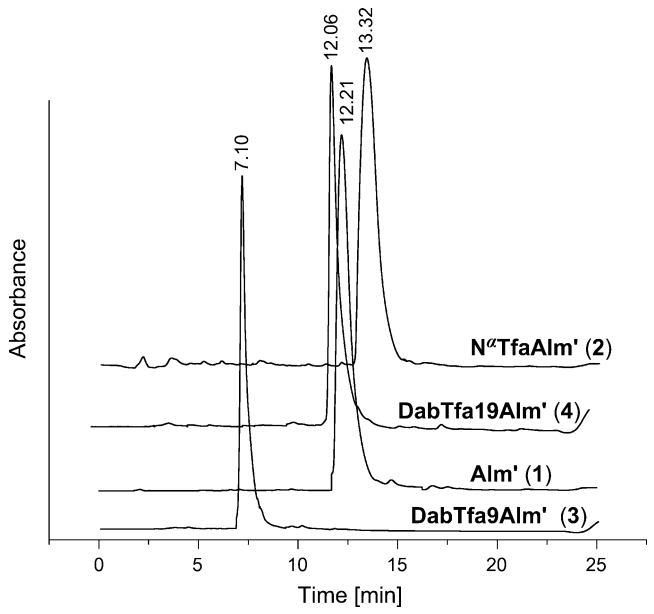

Fig. 1. *Analytical RP-HPLC elution profiles* (retention times (t_R)) *of the three Tfa-containing* **Alm′** (**1**) *analogs.* The profile of **Alm′** (**1**; t_R, 12.21 min) is shown for comparison.

Scheme 3. *Synthesis of* **DabTfa9Alm′ (3)**

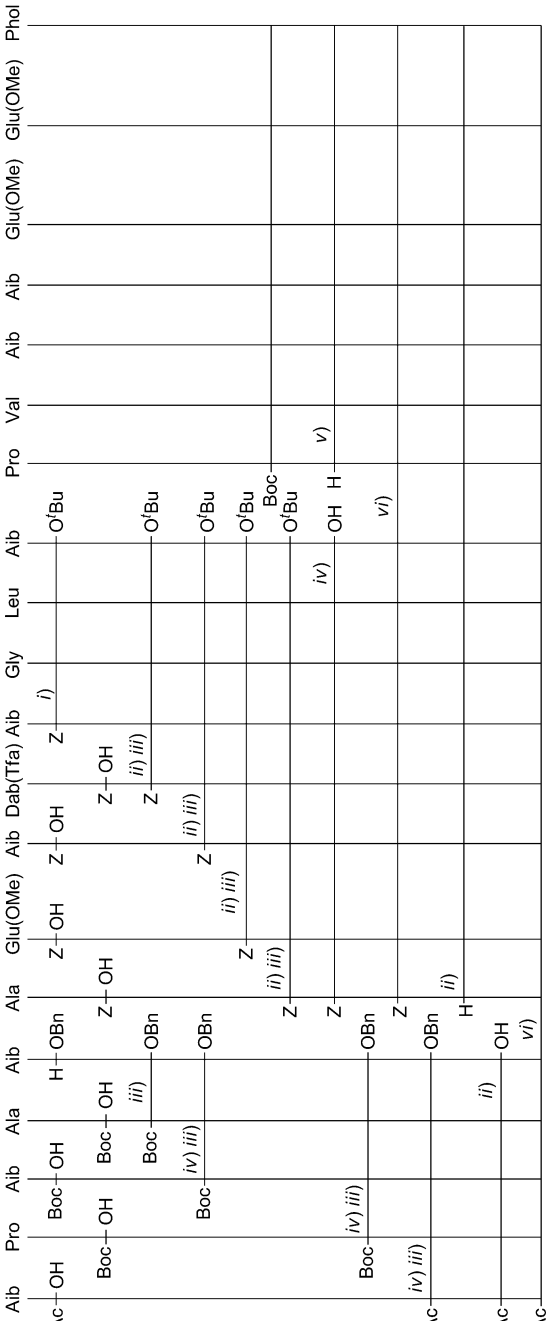

i) See [30]. *ii*) H_2/Pd, MeOH. *iii*) EDC/HOAt, NMM (to keep pH 8). *iv*) 10 equiv. of TFA, anh. CH_2Cl_2. *v*) 10 equiv. of TFA, CH_2Cl_2 (removal of the *N*-protecting Boc from the C-terminal segment obtained as described in *Scheme 1*). *vi*) EDC/HOAt, NMM (to keep pH 8).

Scheme 4. *Synthesis of* **DabTfa19Alm′ (4)**

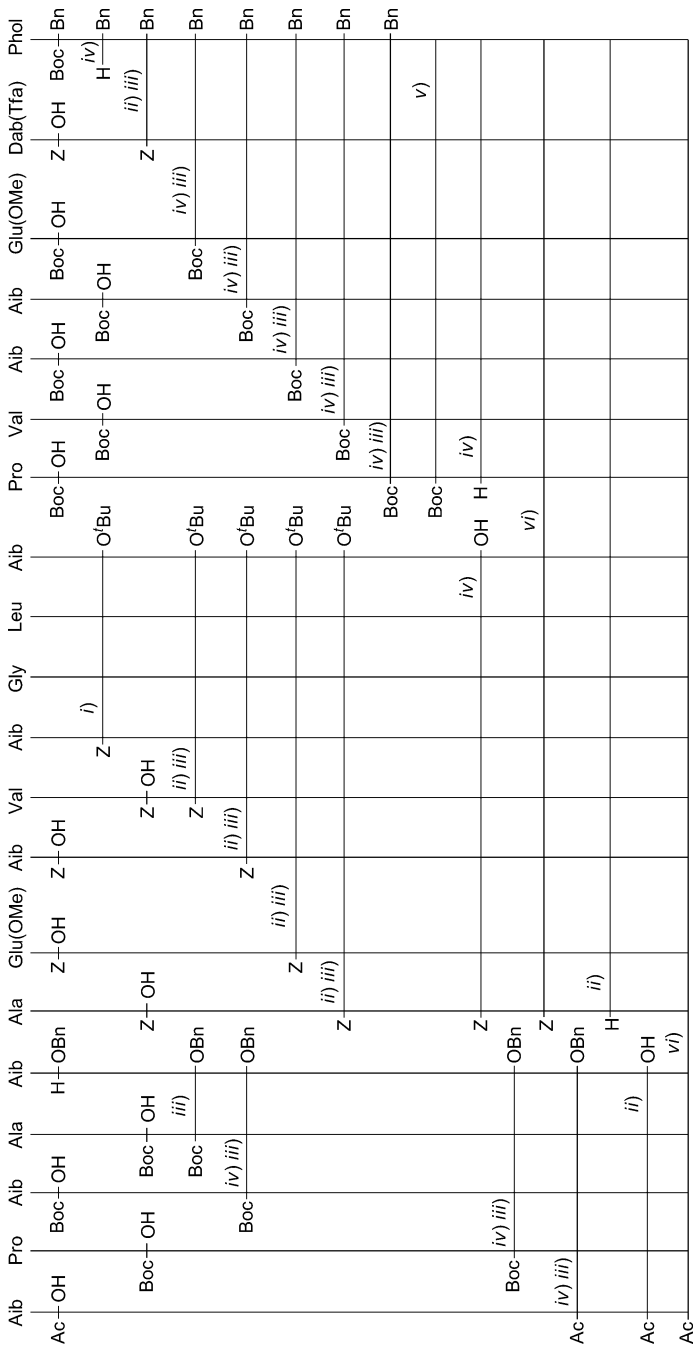

i) See [30]. *ii*) H_2/Pd, MeOH, 30 min. *iii*) EDC/HOAt, NMM (to keep pH 8). *iv*) 10 equiv. of TFA, anh. CH_2Cl_2. *v*) H_2/Pd, MeOH, 5 d. *vi*) EDC/HOAt, NMM (to keep pH 8).

Tfa in the central position of the sequence (**DabTfa9Alm′** (**3**)) appears to be markedly less hydrophobic than its two congeners and the parent peptide (**Alm′**). Additional characterizations of the final peptaibiotics include solid-state FT-IR absorption, ^{1}H- and ^{13}C-NMR, and ESI-TOF-MS data.

IR Absorption. The conformational preferences of the three Tfa-labeled peptides were initially investigated by FT-IR spectroscopy in $CDCl_3$ solution. In *Fig. 2*, the amide A (*a*) and amide I/II (*b*) regions, recorded for the peptides at 1 mM concentration, are displayed along with those of **Alm′** (**1**) [29], shown for comparison. In *Fig. 2, b*, the spectral intensities were normalized on the amide II band at 1538 cm^{-1}. The amide A regions of all peptides analyzed were dominated by a strong band at *ca.* 3320 cm^{-1}, that we assigned to the N–H stretching mode of H-bonded –CO–NH– groups [64][65]. A slightly different behavior was exhibited by **N$^{\alpha}$TfaAlm′** (**2**), the corresponding intense band of which was shifted to 3330 cm^{-1}. Also, the weak absorption generally observed at *ca.* 3430 cm^{-1}, associated with free (solvated) amide

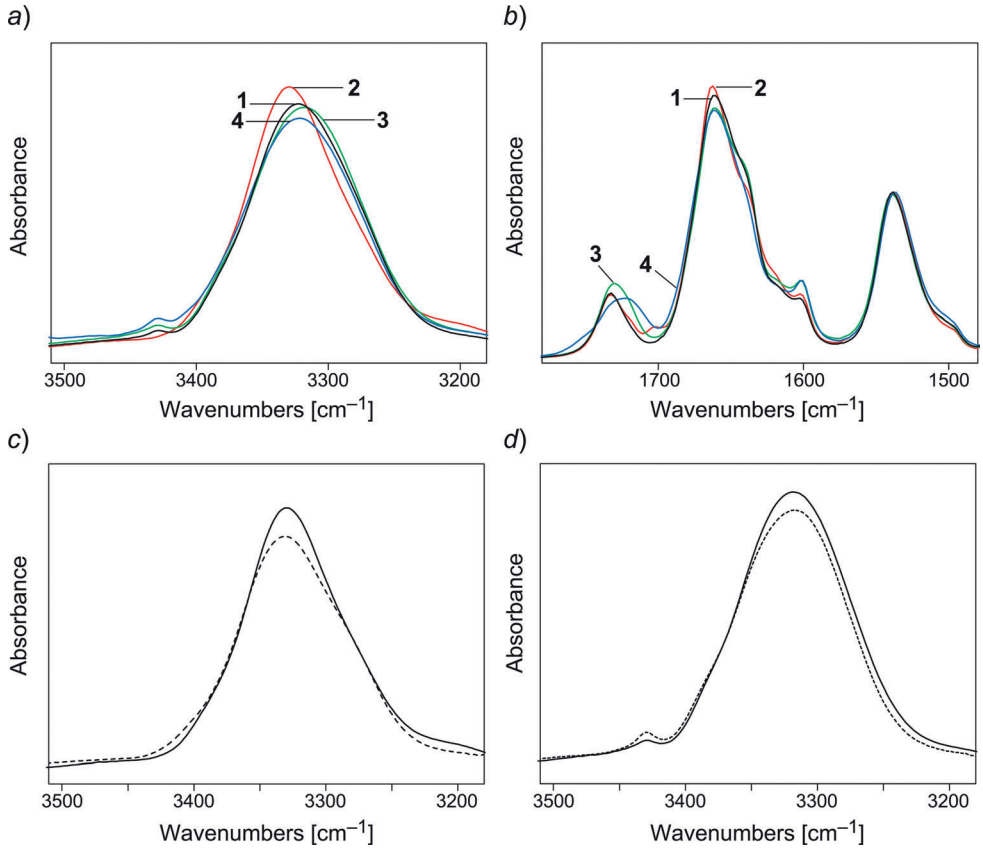

Fig. 2. *FT-IR Absorption spectra in* a) *3500–3200-cm^{-1} region and* b) *1750–1500-cm^{-1} region in $CDCl_3$ solution* (peptide concentration, 1 mM) *of* **Alm′** (**1**), **N$^{\alpha}$TfaAlm′** (**2**), **DabTfa9Alm′** (**3**), *and* **DabTfa19Alm′** (**4**). Effect of peptide concentration in $CDCl_3$ for *c*) **N$^{\alpha}$TfaAlm′** (**2**) and *d*) **DabTfa9Alm′** (**3**): 1 mM (*full line*) and 0.1 mM (*dashed line*).

groups, was completely absent in the spectrum of **N$^{\alpha}$TfaAlm′** (**2**). The dilution effect on the amide A band, illustrated in *Fig. 2, c* and *d*, for two of the peptides, highlights the presence of a highly folded conformation extensively stabilized by a large number of intramolecular H-bonds at the lowest concentration (0.1 mM) examined. Nonetheless, a contribution, albeit modest, of intermolecular N–H···O=C interactions was also apparent.

The position of the intense C=O stretching mode (amide I) near 1655 cm^{-1} (*Fig. 2, b*) in all of the analyzed spectra strongly supports the view that the conformation preferentially adopted by all of the peptides investigated in $CDCl_3$ was of the 3_{10}-/α-helical type [66].

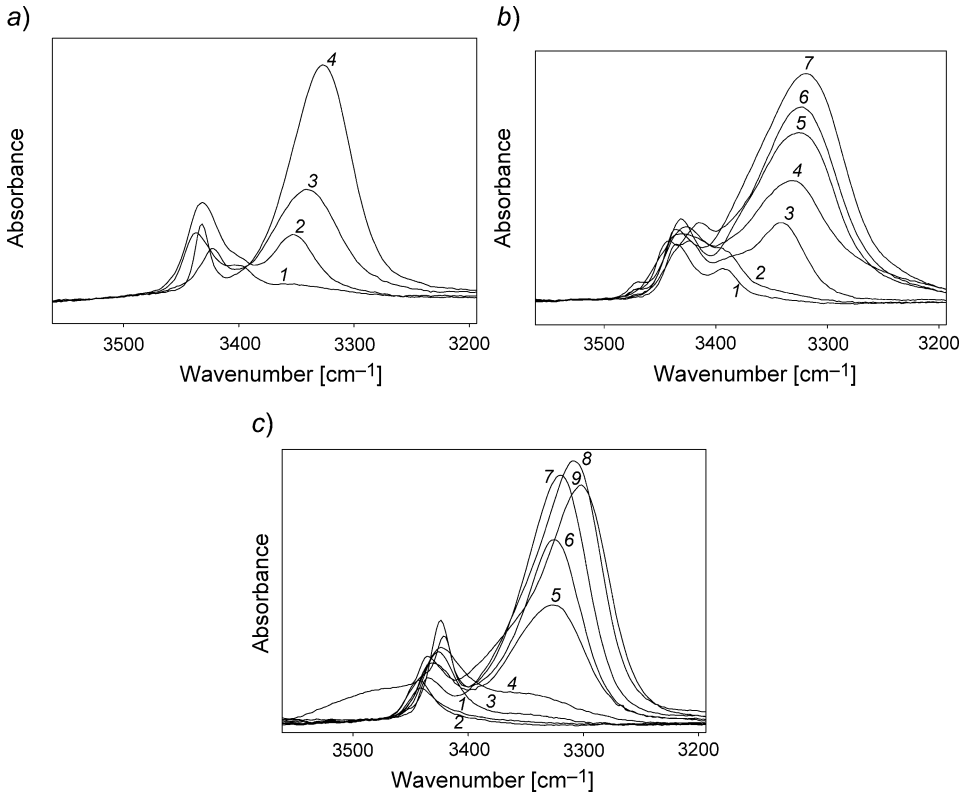

Fig. 3. *FT-IR Absorption spectra in 3500–3200-cm^{-1} region in $CDCl_3$ solution for three sets of representative short sequences. a*) Boc-Ala-Aib-OBn (*1*); Boc-Aib-Ala-Aib-OBn (*2*); Boc-Pro-Aib-Ala-Aib-OBn (*3*); Ac-Aib-Pro-Aib-Ala-Aib-OBn (**5**; *4*). *b*) Z-Leu-Aib-O^{t}Bu (*1*); Z-Gly-Leu-Aib-O^{t}Bu (*2*); Z-Aib-Gly-Leu-Aib-O^{t}Bu (*3*); Z-Dab(Tfa)-Aib-Gly-Leu-Aib-O^{t}Bu (*4*); Z-Aib-Dab(Tfa)-Aib-Gly-Leu-Aib-O^{t}Bu (**6**; *5*); Z-Glu(OMe)-Aib-Dab(Tfa)-Aib-Gly-Leu-Aib-O^{t}Bu (*6*); Z-Ala-Glu(OMe)-Aib-Dab(Tfa)-Aib-Gly-Leu-Aib-O^{t}Bu (*7*). *c*) Boc-Phol (*1*); Boc-Phol(Bn) (*2*); Boc-Glu(OMe)-Phol(Bn) (*3*); Boc-[Glu(OMe)]$_2$-Phol(Bn) (*4*); Boc-Aib-[Glu(OMe)]$_2$-Phol(Bn) (*5*); Boc-(Aib)$_2$-[Glu(OMe)]$_2$-Phol(Bn) (*6*); Boc-Val-(Aib)$_2$-[Glu(OMe)]$_2$-Phol(Bn) (*7*); Boc-Pro-Val-(Aib)$_2$-[Glu(OMe)]$_2$-Phol(Bn) (*8*); Boc-Pro-Val-(Aib)$_2$-[Glu(OMe)]$_2$-Phol (*9*). Peptide concentration, 1 mM.

To follow the onset of the folded conformation as a function of increasing peptide main-chain length, we recorded the FT-IR absorption spectra of three sets of representative short sequences in $CDCl_3$ solution. *Fig. 3* (amide A region) shows that the intramolecularly H-bonded, folded conformation was already present at a level as low as that of the pentapeptides and further developed in the longer sequences, with a much more significantly growing structuration closely related to the percentage of the helix-inducing Aib residues.

Circular Dichroism. The far-UV/CD spectra of the three final Tfa-containing peptides in MeOH and 100 mM sodium dodecylsulfate (SDS) in H_2O (a membrane-mimicking environment) are shown in *Fig. 4, a* and *b*, respectively, together with those of **Alm′** (**1**). Acquisition of the near-UV absorption spectra in the same solvents allowed us to normalize the peptide concentrations, even though only the modest aromatic chromophore of Phol is present in the sequences [67]. Under each of the two experimental conditions examined, all analogs exhibited similar spectral shapes. We have already reported [29] that **Alm** and **Alm′** (**1**) show almost the same CD curves in MeOH. All these CD spectra are indicative of a right-handed, predominantly α-helical structure [68] as the *R* ratio [69–71] between the intensities of the two negative bands at 222 and 208 nm is 0.80 ± 0.05. The population of 3_{10}-helix segments was definitely lower [10][72–74]. In the presence of SDS micelles, the intensity of the negative maximum at 222 nm increased, becoming higher than that at 208 nm (*R* value $1.03 \pm$

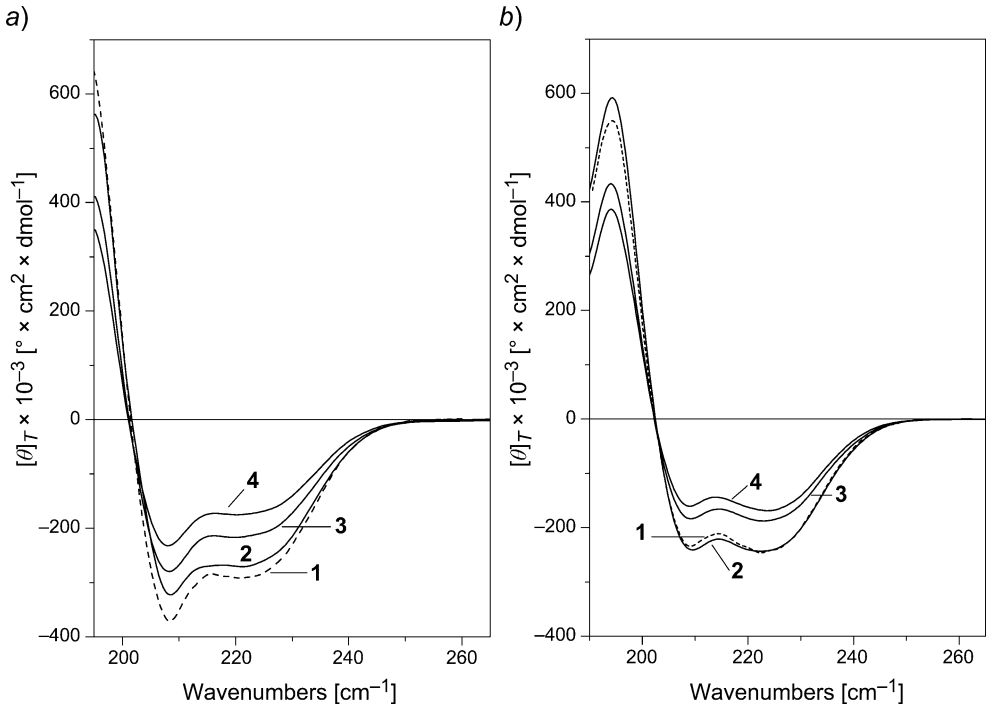

Fig. 4. *Far-UV/CD Spectra for* **Alm′** (**1**), **N$^{\alpha}$TfaAlm′** (**2**), **DabTfa9Alm′** (**3**), *and* **DabTfa19Alm′** (**4**) *in* a) *MeOH and* b) *100 mM SDS solution*. Peptide concentration, 0.1 mM.

0.02). This observation strongly suggests the onset of an extremely well-developed α-helical structure in this membrane-mimicking environment for all of the peptides investigated. We conclude that neither the presence of a non-proteinogenic α-amino acid (Dab) bearing a side-chain Tfa probe nor the replacement of the N-terminal capping group (Ac) with Tfa affects dramatically the overall peptide conformation in the two environments of different polarity investigated.

NMR Spectroscopy. We extended our conformational analysis of the Tfa-labeled analogs of **Alm′** (**1**) in CD_3OH solution by using the 2D-NMR technique. Despite the length of the peptide sequence and the occurrence of many amino acids of the same type (*e.g.*, eight Aib residues) and two Pro (lacking the NH H-atom) the assignment of all of the H-atom resonances was successfully achieved by exploiting the standard *Wüthrich* procedure [75], supported by the 2D HMBC spectrum [76]. Several NOESY spectra were acquired at different mixing times. Eventually, the mixing time of 250 ms was chosen, as it provided the best signal-to-noise ratio without the presence of spin-diffusion effects.

As a typical example, two portions of the NOESY spectrum of **DabTfa9Alm′** (**3**) are shown in *Figs. 5* and *6*. The presence of all NH_i-NH_{i+1} cross-peaks (*Fig. 5*), except those covered by the diagonal peaks, along with a number of $C^{\alpha}H_i \rightarrow NH_{i+1}$ and $C^{\alpha}H_i \rightarrow$

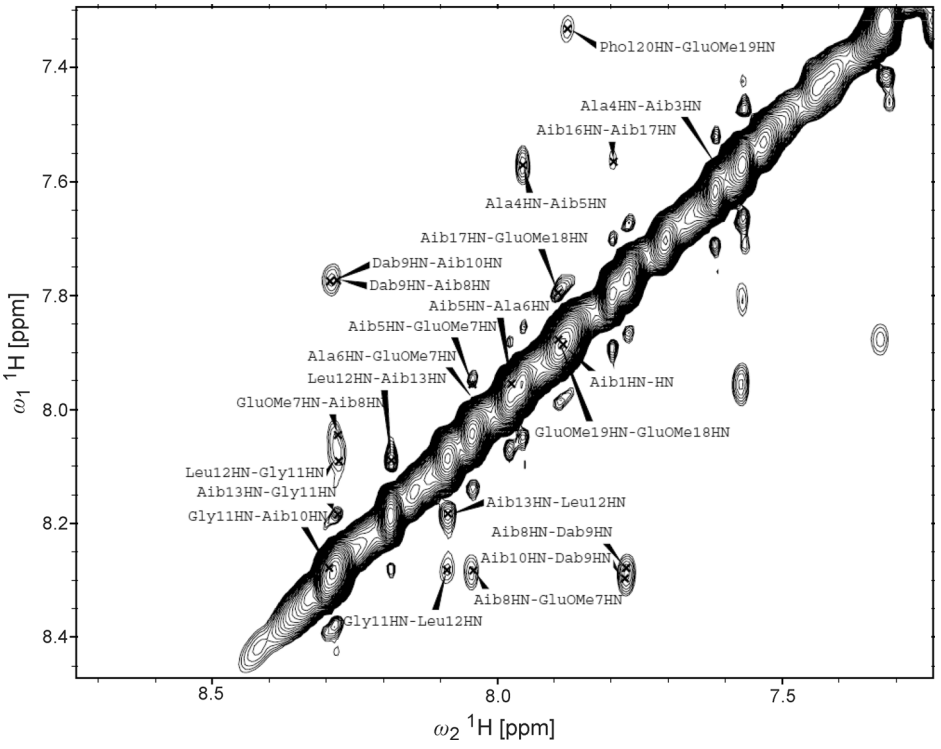

Fig. 5. *Section* (amide NH H-atom region) *of the NOESY spectrum of* **DabTfa9Alm′** (**3**) *in CD_3OH solution* (600 MHz, 298 K). Peptide concentration, 1.64 mM.

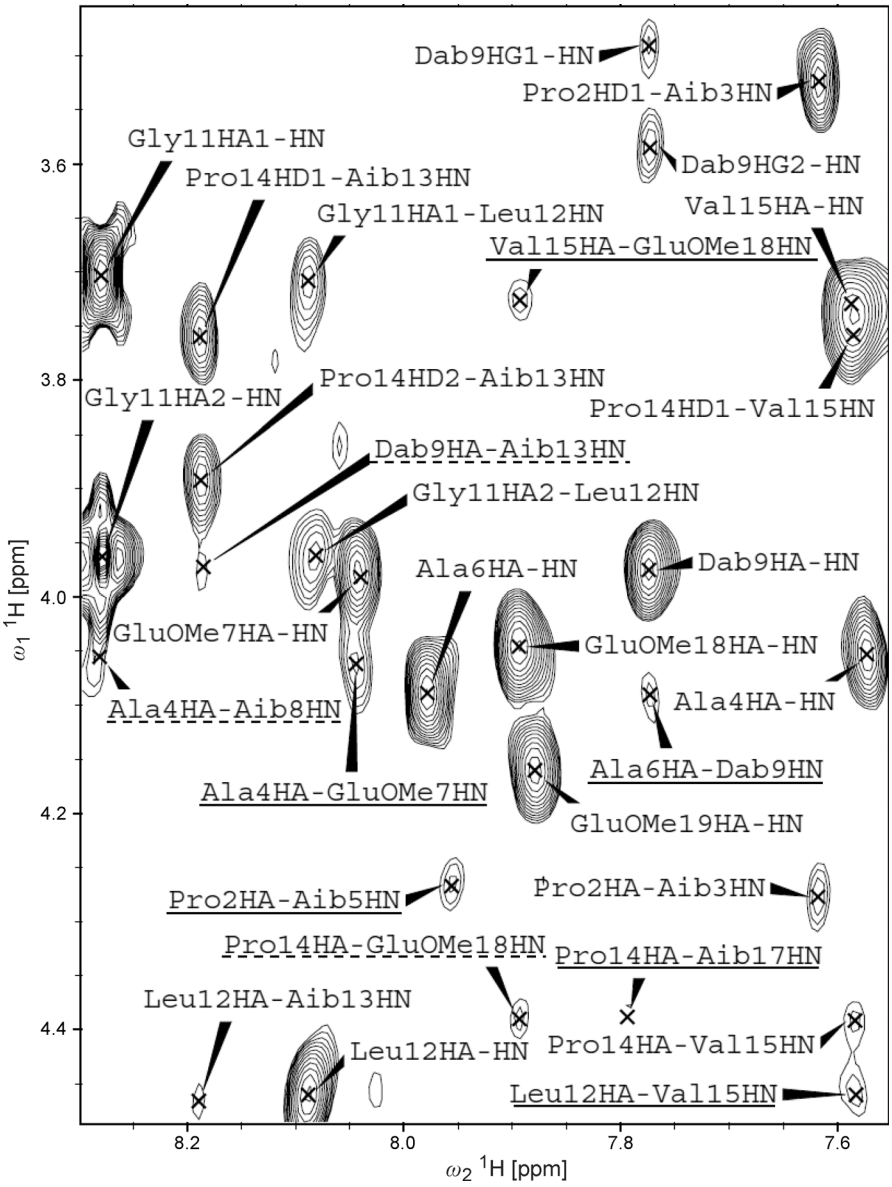

Fig. 6. *Fingerprint region of the NOESY spectrum of* **DabTfa9Alm′** (**3**) *in* CD_3OH *solution* (600 MHz, 298 K). Peptide concentration, 1.64 mM. The medium-range connectivities $C^{\alpha}H_i \rightarrow NH_{i+3}$ (*full line*) and $C^{\alpha}H_i \rightarrow NH_{i+4}$ (*dashed line*) are underlined.

NH_{i+3} connectivities (*Fig. 6*), highlights the occurrence of a well-defined, helical structure throughout the amino acid sequence. Furthermore, the detection of several $C^{\alpha}H_i \rightarrow NH_{i+4}$ medium-length connectivities, well spread all over the sequence (*Fig. 6*), allowed us to conclude that **DabTfa9Alm′** (**3**) is folded in a largely α-helical

conformation, closely resembling that of the parent peptide [32]. The corresponding NOESY spectra for the other two trifluoroacetylated analogs (deposited) indicated that the overall prevaling α-helical conformation was largely mantained.

X-Ray Diffraction. A variety of attempts to grow single crystals appropriate for an X-ray diffraction analysis allowed us to solve the 3D structures of the terminally protected pentapeptide ester Ac-Aib-Pro-Aib-Ala-Aib-OBn (**5**), hexapeptide ester Z-Aib-Dab(Tfa)-Aib-Gly-Leu-Aib-O^{t}Bu (**6**), and the tetrapeptide amide Boc-$(Aib)_2$-Glu(OMe)-Dab(Tfa)-Phol(Bn) (**7**; *Fig. 7*). These compounds represent the N-terminal, central (residues 8–13), and C-terminal sequences, respectively, of the **Alm** analogs synthesized in this work. The most relevant conformational and intramolecular H-bond parameters for the three oligopeptides are compiled in *Tables 2* and *3*, respectively.

Bond lengths and bond angles (deposited) are in general agreement with previously reported values for the geometry of the Boc-NH– [77] and Z-NH– [78] urethane moieties, the peptide unit [79][80], the methyl/benzyl ester group [81], and the Aib [82][83] residue.

In the four molecules of the three peptides, all amide/peptide bonds (ω torsion angles) are in the common *trans* disposition [79][80]. The conformation of the peptide backbone (φ, ψ torsion angles) of the pentapeptide ester **5** is helical, stabilized by two strong and one weak intramolecular C=O···H–N H-bonds [84–86]. From the N-terminus of the main chain, two strong H-bonds are formed by the Aib^{3}NH and Ala^{4}NH groups as donors, and the Ac and Aib^{1}C=O groups as acceptors, respectively. Rather unusually, the Aib^{1}C=O group is the acceptor of a further, weak H-bond, from the Aib^{5}NH group as the donor. Collectively, the intramolecular H-bonding scheme is characterized by two consecutive C_{10} (β-turn [87–89]) forms (incipient 3_{10}-helix [72][73]), the second of which is embraced by a larger C_{13} (α-turn [88][90]) form. This latter conformation is generated by the wide φ torsion angle, observed for the Ala^4 residue. Also the C-terminal Aib^5 residue, partially external to the helix structure, is helical, but its screw sense is opposite to that of the preceding residues. This is a common observation for 3_{10}-helical peptide esters with a C-terminal $C^{\alpha,\alpha}$-dialkyl glycine [91]. The pyrrolidine ring of the Pro residue has a symmetry between twist $^4T_3$ and ^4E [92][93] with ring-puckering parameters [94] $q_2 = 0.380(7)$ Å and $\varphi_2 = -81.6(7)^\circ$.

Two helical, but conformationally distinct molecules **6A** and **6B** (*Fig. 7*) occur in the asymmetric unit of the hexapeptide ester **6**. Not only some of the χ torsion angles of the long side chains of Dab(Tfa)^2 and Leu^5 residues (deposited) differ remarkably, but a few main-chain φ, ψ torsion angles as well. Notably, the φ values for Gly^4 and Leu^5, both in molecule **6A**, and for Leu^5 in molecule **6B** are considerably expanded, although to a different extent, from the regular helical values. Moreover, the ψ values for Gly^4 in molecules **6A** and **6B**, and particularly for Dab(Tfa)^2 in **6B** are very compressed. As a result, the four intramolecular C=O···H–N H-bonds in molecule **6B** are those expected for a 3_{10}-helix, whereas those in molecule **6A** are not. Indeed, the N6–H···O3 H-bond (C_{10} form), which should have characterized the 3_{10}-helix of molecule **6B**, is missing, and it is replaced by a N6–H···O2 H-bond (C_{13} form). Here too, as already highlighted above for **5**, near the C-terminus, a C=O O-atom (the O2 atom in this case) is a double acceptor of intramolecular H-bonds. Again, in both molecules **6A** and **6B**, the screw sense of the C-terminal helical Aib residue is opposite to that of the preceding

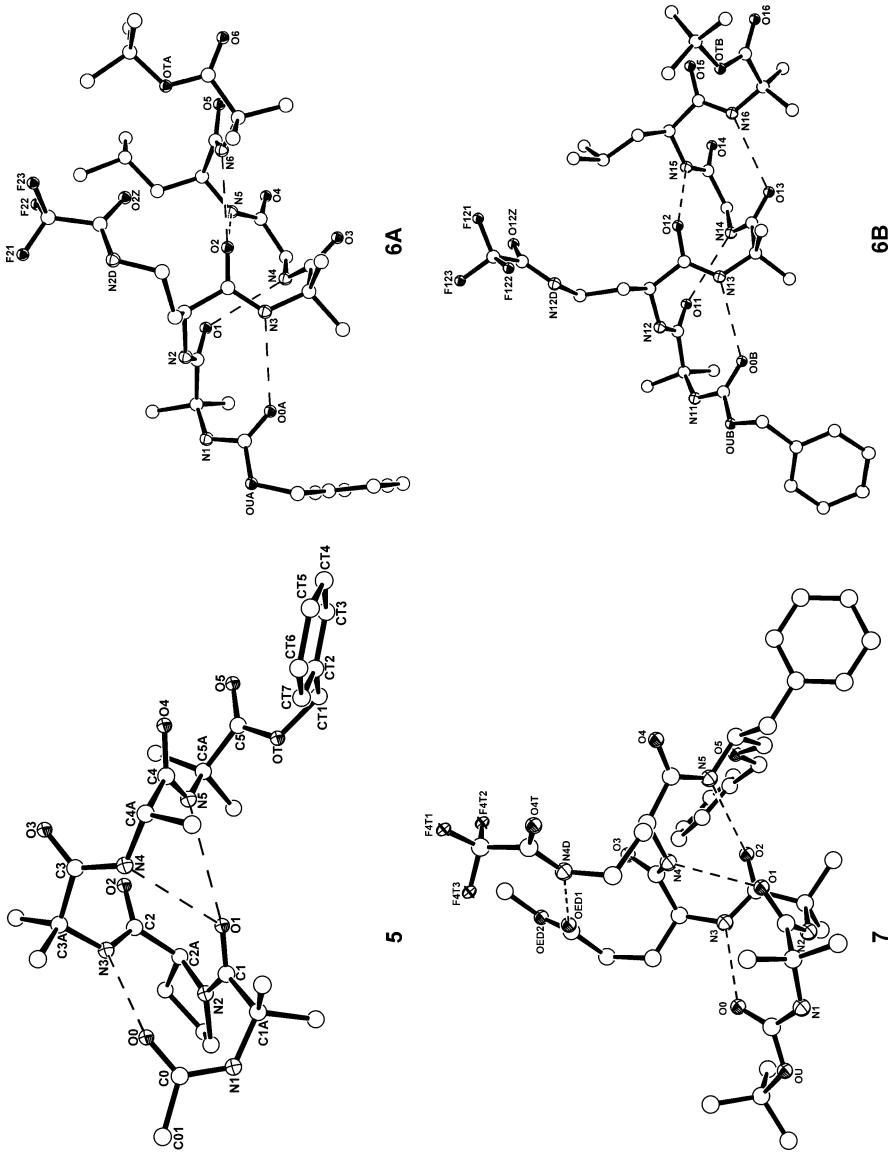

Fig. 7. *X-Ray diffraction structures of Ac-Aib-Pro-Aib-Ala-Aib-OBn* (**5**), *the two independent molecules in the asymmetric unit of Z-Aib-Dab(Tfa)-Aib-Gly-Leu-Aib-O'Bu* (**6**), *and Boc-(Aib)$_2$-Glu(OMe)-Dab(Tfa)-Phol(Bn)* (**7**) *with atom numberings.* The intramolecular C=O···H–N H-bonds are represented by dashed lines. Note that in **7** one of the H-bonds involves a side chain-to-side chain interaction. Only one position for each of the disordered Tfa group and the Dab side chain of the molecule **6B** *d*) is shown. Only the major conformer for the disordered Tfa group of the molecule shown in **7** is displayed.

Table 2. *Backbone Torsion Angles for Peptides* **5**–**7**

Residue	**5**			Residue	**7**		
	φ [°]	ψ [°]	ω [°]		φ [°]	ψ [°]	ω [°]
Aib[1]	−52.8(6)	−37.4(6)	−178.3(4)	Aib[1]	−54.5(6)	−30.7(6)	179.5(4)
Pro[2]	−58.3(5)	−29.5(6)	179.4(4)	Aib[2]	−45.2(6)	−39.9(6)	−171.2(4)
Aib[3]	−55.4(6)	−38.6(5)	−178.8(4)	Glu(OMe)[3]	−57.8(6)	−30.7(6)	−177.1(4)
Ala[4]	−78.2(5)	−34.1(6)	173.5(5)	Dab(Tfa)[4]	−87.8(5)	−4.7(7)	−175.2(4)
Aib[5]	52.2(8)	48.7(7)	173.7(6)				
Residue	Molecule **6A**				Molecule **6B**		
	φ [°]	ψ [°]	ω [°]		φ [°]	ψ [°]	ω [°]
Aib[1]	−60.5(6)	−31.5(6)	−178.2(4)		−52.1(6)	−39.2(6)	−174.1(5)
Dab(Tfa)[2]	−52.2(6)	−34.6(5)	−174.7(4)		−67.2(6)	−8.4(7)	167.9(5)
Aib[3]	−60.2(6)	−26.4(6)	179.7(4)		−51.4(8)	−29.6(8)	179.7(6)
Gly[4]	−82.9(6)	−17.0(7)	−176.8(5)		−61.6(8)	−19.4(8)	175.0(5)
Leu[5]	−99.7(6)	−54.8(6)	176.4(5)		−68.6(6)	−25.1(6)	−177.2(5)
Aib[5]	54.2(7)	46.5(6)	174.7(5)		45.7(7)	46.2(7)	−176.4(5)

Table 3. *Intramolecular H-Bond Parameters for Peptides* **5**–**7**

Donor D–H	Acceptor A	Distance [Å] D···A	Distance [Å] H···A	Angle [°] D–H···A
5				
N3–H	O0	3.041(6)	2.28	147
N4–H	O1	2.984(5)	2.29	138
N5–H	O1	3.337(5)	2.51	163
6				
N3–H	O0**A**	3.070(5)	2.25	159
N4–H	O1	2.966(5)	2.18	152
N5–H	O2	3.054(5)	2.26	153
N6–H	O2	3.038(5)	2.22	159
N13–H	O0**B**	3.018(7)	2.18	163
N14–H	O11	3.012(6)	2.16	169
N15–H	O12	2.907(6)	2.07	164
N16–H	O13	3.020(6)	2.22	155
7				
N3–H	O0	2.982(5)	2.14	165
N4–H	O1	3.026(5)	2.24	153
N5–H	O2	3.029(5)	2.20	163
N4D–H	O3E1	2.920(6)	2.11	156

residues. Finally, in both molecules, the Dab side-chain trifluoroacetamide NH group is intermolecularly H-bonded to a corresponding peptide C=O O-atom of a molecule related by the same symmetry operation.

The backbone of **7** (*Fig. 7*) is folded in a (partially irregular) 3_{10}-helical structure with three strong intramolecular C=O···H–N H-bonds. The donors of the C_{10} forms

are the main-chain Glu(OMe)[3], Dab(Tfa)[4], and Phol C-terminal amide NH groups, and the acceptors are the Boc urethane and the peptide C=O groups of the Aib[1] and Aib[2] residues. The C-terminal β-turn is type I [87–89], produced by the non-helical φ, ψ values of the Dab(Tfa)[4] residue. A surprising, previously unreported in crystalline peptides, property of this 3D structure is the occurrence of an additional intramolecular C=O···H–N H-bond which links the two long, functionalized side chains of the consecutive Glu(OMe)[3] and Dab(Tfa)[4] residues. The former affords the methyl ester C=O acceptor, and the latter acts as the trifluoroacetamido N–H donor. The crystal packing modes and intermolecular H-bondings for peptides **5**–**7** are presented and discussed in the *Supplementary Information* (available upon request from the authors).

To summarize our results in the crystalline state, the three short peptides are extensively folded in helical structures. This 3D-structural disposition is associated with the remarkable amount ($\geq$50%) of Aib residues in the sequences [10][72][73]. Not surprisingly, in view of the limited length (<seven residues) of the peptides [10][72][73], the helix adopted is primarily of the 3_{10}-type, although with minor irregularities near the C-terminus. A comparison among the 3D structures reported above, and the conformations of the corresponding 1–5-, 8–13-, and 16–19-Phol peptide segments in the published full-length X-ray structures of **Alm** (three crystallographically independent molecules) [20] and its (Glu(OMe)[7,18,19], TOAC[16]) (TOAC = 4-amino-2,2,6,6-tetramethyl-1-oxylpiperidine-4-carboxylic acid) analog (two independent molecules) [38] indicates an overall conformational similarity, in that these segments are also helical in the full-length molecules. Differences, however, are found in the details of the H-bonding patterns (C_{10} *vs.* C_{13} forms, C_{10} forms encompassed within C_{13} forms). The most notable difference is found for the 8–13 segment (*Fig. 7*), which is mainly (molecule **6A**) or fully (molecule **6B**) 3_{10}-helical in the structure of **6** reported in this work, whereas it shows an almost exclusive α-helical character when part of **Alm** or its (Glu(OMe)[7,18,19], TOAC[16]) analog. A mixed α-/3_{10}-helical structure was also observed for **Alm** when reconstituted into a supported POPC (1-palmitoyl-2-oleoyl-*sn*-glycero-3-phosphocholine) phospholipid bilayer by using solid-state ^{15}N-NMR spectroscopy [95].

Solid-State ^{19}F-NMR Spectroscopy. As a result of an initial MAS (magic angle spinning) solid-state ^{19}F-NMR analysis, the spectrum of a sample of **N$^{\alpha}$TfaAlm′** (**2**) reconstituted in a POPC bilayer and recorded in the frozen state is shown in *Fig. 8, a*. The chemical-shift anisotropy of 40 ppm allows for the magnetization exchange between magnetically inequivalent CF_3 groups as they occur for chemically equivalent peptide molecules in an oligomeric aggregate (*Fig. 8, b*). The normalized magnetization exchange curve (S/S_0 in *Fig. 8, b*) is indicative of the presence of oligomers.

Antimicrobial Activity. The antimicrobial activities of the three trifluoroacetylated analogs of **Alm′** (**1**) were assessed on *Gram*-positive (*Staphylococcus aureus* and *Enterococcus faecalis*) and *Gram*-negative (*Escherichia coli*, *Yersinia enterocolitica*, and *Shigella flexneri*) bacteria, and on the fungus *Candida albicans*, and were compared to those of the parent compound **Alm′** (**1**; *Table 4*). The most interesting results are those of **DabTfa19Alm′** (**4**) which exhibits a broad spectrum of action including against both *Gram*-positive and *Gram*-negative bacteria. This finding is at variance with those obtained for **N$^{\alpha}$TfaAlm′** (**2**), **DabTfa9Alm′** (**3**), and **Alm′** (**1**) (the latter appreciably active only on the thick *cellular* wall of the *Gram*-positive *E. faecalis* strain), all of

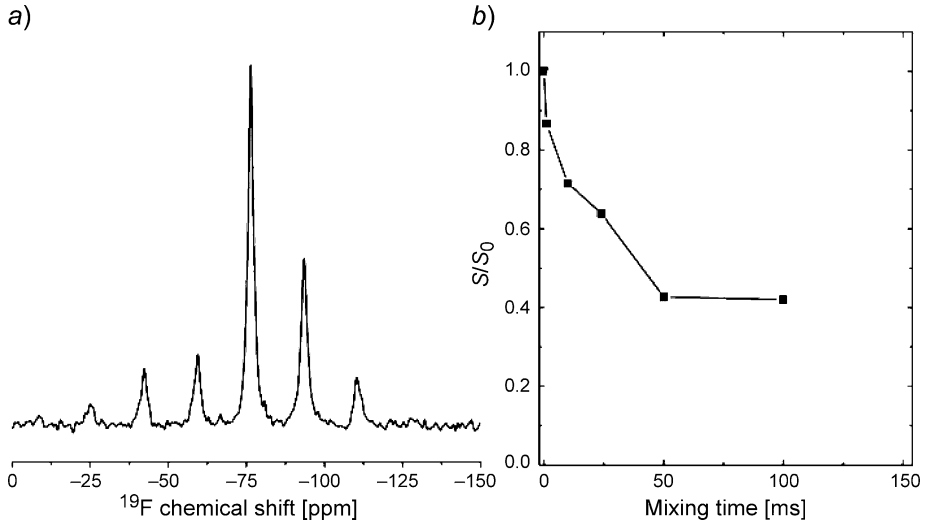

Fig. 8. a) *Experimental solid-state [19]F-NMR spectrum of 11 mol-%* **N$^{\alpha}$TfaAlm′** (**2**) *in POPC* (=1-palmitoyl-2-oleoyl-*sn*-glycero-3-phosphocholine) *at* $-25°$. The MAS (magic angle spinning) frequency is 8 kHz. The resulting spinning side bands reveal the chemical-shift anisotropy. *b*) Experimental CODEX curve obtained at a MAS frequency of 15 kHz. The data points are indicated by black squares (uncertainty ± 0.2).

Table 4. *Antimicrobial Activities of Peptides* **Alm′** (**1**), **N$^{\alpha}$TfaAlm′** (**2**), **DabTfa9Alm′** (**3**), *and* **DabTfa19Alm′** (**4**) (at 100 μg/disk)[a])

Bacterial strain	**Alm′** (**1**)	**N$^{\alpha}$TfaAlm′** (**2**)	**DabTfa9Alm′** (**3**)	**DabTfa19Alm′** (**4**)
Staphylococcus aureus ATCC 25923	6	6	6	6
Enterococcus faecalis ATCC 29212	9	7	7	8
Escherichia coli ATCC 25922	6	6	6	8
Yersinia enterocolitica ATCC 27739	6	6	6	10
Shigella flexneri clinical isolate	6	6	6	7
Candida albicans ATCC 1028	6	6	6	6

[a]) Diameter of inhibition zone ([mm]).

which appear to be unable to penetrate the highly selective *external* membrane of the *Gram*-negative bacterial cells. For a comparison with the related antimicrobial activities of the **Alm** natural mixture, the reader is referred to [26]. Since these Tfa-labeled peptaibiotics are potentially toxic compounds, it is not superfluous to remind that their syntheses were exclusively aimed towards a solid-state [19]F-NMR investigation.

Conclusions. – Peptaibiotics bind to lipid membranes and self-associate into oligomers. The solid-state [19]F-NMR technique provides in-depth information about the 3D structure, dynamics, and topology of peptides incorporated into membranes. We are currently investigating this biophysical phenomenon in F-labeled analogs of the long

(19 amino acid residues), highly helical peptaibiotic **Alm** which forms channels in the phospholipid membranes [46][57].

In this contribution, we described the solution-phase synthesis and chemical characterization of three such peptaibiotics, each containing a single Tfa probe either at the N-terminus, in the central region, or near the C-terminus, respectively. To this end, we partially modified our previously published synthetic schemes of **Alm** and some of its analogs [29][30] with beneficial effects. We demonstrated by a number of spectroscopic techniques (FT-IR absorption, CD, and NMR) in SDS micelles, in organic solvents of different polarity ($CDCl_3$ and MeOH), and in the crystalline state (by X-ray diffraction analyses of three segments spanning almost entirely the **Alm′** (**1**) amino acid sequence) as well that the typical helical properties of this peptaibiotic [29][30][32] are essentially preserved, *i.e.*, that the herein described **Alm′** (**1**) ^{19}F-labeling strategy is conformationally harmless. Our initial solid-state ^{19}F-NMR investigation on the **N$^{\alpha}$TfaAlm′** (**2**) analog unambiguously indicated the formation of oligomeric aggregates when this peptide is immersed into a phospholipid membrane. All three trifluoroacetylated analogs of **Alm′** (**1**) are antimicrobially active, although with partially different specific properties.

This work was supported by the *Italian Ministry of Education, University, and Research, MIUR* (grant PRIN 2008).

Experimental Part

General. Amino acids and their derivatives were purchased from *IRIS Biotech*. *N*-Ethyl-*N*′-[3-(dimethylamino)propyl]carbodiimide (EDC) and 1-hydroxy-7-aza-1,2,3-benzotriazole (HOAt) [96] were *GL Biochem* products. All chiral amino acids employed are of the L-configuration. All other chemicals were obtained from *Sigma–Aldrich*. The final products were analyzed by anal. RP-HPLC on a *Jupiter Phenomenex* C_4 column (4.6 × 250 mm, 5 μm, 300 Å) using an *Agilent 1200* HPLC pump. The binary elution system used was: *A*, H_2O/MeCN 9 : 1; *B*, MeCN/H_2O 9 : 1; gradient 60–80% *B* in 20 min (flow rate 1 ml/min); spectrophotometric detection at λ 226 nm. Anal. TLC and prep. column chromatography (CC): *Kieselgel* F_{254} and *Kieselgel 60* (0.040–0.063 mm; *Merck*), resp. The retention factor (R_f) values were determined using four solvent mixtures as eluants: R_{f1}: $CHCl_3$/ EtOH 9 : 1; R_{f2}: BuOH/AcOH/H_2O 3 : 1 : 1; R_{f3}: toluene/EtOH 7 : 1; R_{f4}: CH_2Cl_2/ MeOH 98 : 2. M.p.: Cap. tube immersed in an oil bath (*Tottoli apparatus*, *Büchi*); uncorrected. ESI-TOF-MS: *PerSeptive Biosystem Mariner* instrument; in *m*/*z*.

CD Experiments. CD Recordings were carried out on a *JASCO J-715* spectropolarimeter. The CD spectra were acquired and processed using the J-700 program for *Windows*. All spectra were recorded at r.t., using *Hellma* quartz cells with *Suprasil*® windows and optical path length of 0.1 cm. The signal-to-noise ratio was improved by accumulating eight scans. The values are expressed in terms of total molar ellipticity, $[\theta]_T$ [degree · cm^2 · dmol^{-1}]. Spectrograde MeOH (99.9%) and 100 mM aq. SDS soln. were used as solvents.

FT-IR Absorption Experiments. The FT-IR absorption spectra were recorded with a *PerkinElmer 1720X* spectrophotometer, N_2-flushed, equipped with a sample-shuttle device, at a nominal resolution of 2 cm^{-1}, averaging 100 scans; $\tilde{\nu}$ in cm^{-1}. Solvent (baseline) spectra were obtained under the same conditions. Cells with path lengths of 1.0 and 10 mm (with CaF_2 windows) were used. Spectrograde $CDCl_3$ (99.8%, D) was purchased from *Merck*.

NMR Experiments. 1D ^{1}H- and ^{13}C-NMR spectroscopy was employed to characterize the synthesized compounds. $CDCl_3$ and (D_6)DMSO were used as solvents. All spectra were acquired on a *Bruker Avance DMX-600* or *DRX-400* operating at 600 or 400 MHz, resp., using the TOPSPIN software package; δ in ppm rel. to Me_4Si as internal standard, *J* in Hz. The 2D-NMR experiments were carried out on

DabTfa9Alm′ (**3**; 2 mg of the peptide dissolved in 0.55 ml of CD_3OH; final peptide concentration; 1.6 mM). All experiments were acquired at 298 K on a *Bruker Avance DMX-600* instrument. Suppression of the OH solvent signal was obtained applying a WATERGATE gradient program. The standard *Wüthrich* procedure [75] was employed to obtain the assignment of the spin systems of the trisubstituted residues. The CLEAN-TOCSY [97][98] spectrum (spin lock pulse, 70 ms) was acquired by conducting 400 experiments of 40 scans each, whilst for the NOESY spectrum 400 experiments, each one consisting of 96 scans, were carried out. The sequential assignment was performed by means of NOESY (mixing time, 250 ms) and HMBC [76] (160 t_1 increments of 200 scans each and 2K points; spectral width, 200 ppm, centered at 95 ppm in F1) experiments.

Solid-State ^{19}F-NMR Experiments. A homogeneous mixture of POPC (= 1-palmitoyl-2-oleoyl-*sn*-glycero-3-phosphocholine; *Avanti Polar Lipids*) and **N$^{\alpha}$TfaAlm′** (**2**) at a molar ratio of 1:8 was obtained in $CHCl_3$. The soln. was dried under a flow of N_2 and then left *in vacuo* overnight. The mixture was dispersed in 10 mM *Tris* buffer (pH 7.5) by vortex mixing. Thereafter, the hydrated lipid bilayers were subjected to five rapid freeze thaw cycles, centrifuged, and concentrated by pelleting in a benchtop centrifuge. After removal of the excess buffer, a dense suspension of multilamellar vesicles in H_2O (*ca.* 50% *w/w* H_2O content) was obtained. Solid-state ^{19}F-NMR spectra were acquired at 470.4 MHz on a *Bruker Avance widebore 500 NMR* spectrometer equipped with a triple resonance MAS 3.2 mm probe that allows simultaneous tuning of the ^{1}H and ^{19}F frequencies on a single channel through a combiner/splitter assembly. For the CODEX experiments [45], the spinning speed was set to 15 kHz. Experiments were conducted at −25°. Typical radio frequency (rf) field strengths were 70 and 50 kHz for ^{19}F and ^{1}H, resp. The recycle delay was 1 s. ^{19}F Chemical shifts were referenced to the *Teflon* ^{19}F signal at −122 ppm.

Boc-Phol-Bn. Yield: 90%. M.p. 54–55°. R_{f1}: 0.95, R_{f2}: 0.95, R_{f3}: 0.80, R_{f4}: 0.85. IR (KBr): 3375, 1683, 1517. ^{1}H-NMR (400 MHz, $CDCl_3$): 7.39–7.14 (*m*, 10 arom. H, Bn, Phol); 4.89 (*m*, BocN*H*); 4.49 (*m*, CH_2, Bn); 3.96 (*m*, α-CH, Phol); 3.43–3.37 (*m*, C*H*$_2$O, Phol); 2.94–2.76 (*m*, β-CH_2); 1.43 (*s*, Boc). ^{13}C-NMR (150 MHz, $CDCl_3$): 155.38; 138.27; 129.48; 128.45; 128.39; 127.78; 126.30; 73.25; 70.13; 51.68; 37.91; 28.42. ESI-TOF-MS: 342.20 ($[M+H]^+$; calc. 342.27).

Boc-Glu(OMe)-Phol-Bn. Yield: 80%. M.p. 81–82°. R_{f1} 0.95, R_{f2} 0.95, R_{f3} 0.95, R_{f4} 0.50. IR (KBr): 3350, 3314, 1732, 1683, 1657, 1522. ^{1}H-NMR (400 MHz, $CDCl_3$): 7.37–7.15 (*m*, 10 arom. H, Bn, Phol); 6.48 (*d*, 1 H); 5.18 (*m*, 1 H); 4.50 (*m*, CH_2, Bn); 4.27 (*m*, 1 H); 4.11 (*m*, 1 H); 3.68 (*s*, Glu(O*Me*)); 3.40 (*m*, C*H*$_2$O, Phol); 2.88 (*m*, β-CH_2, Phol); 2.36 (*m*, β-CH_2, Glu(OMe)); 2.05 (*m*, 1 H of γ-CH_2, Glu(OMe)); 1.88 (*m*, 1 H of γ-CH_2, Glu(OMe)); 1.43 (*s*, Boc). ^{13}C-NMR (150 MHz, $CDCl_3$): 173.78; 170.85; 155.63; 137.85; 129.38; 128.46; 127.82; 126.48; 73.27; 69.62; 53.85; 51.81; 50.49; 45.79; 37.48; 30.20; 28.31; 28.02.

Boc-Glu(OMe)-Glu(OMe)-Phol-Bn. Yield: 81%. M.p. 123–124°. R_{f1} 0.95, R_{f2} 0.95, R_{f3} 0.20, R_{f4} 0.95. IR (KBr): 3326, 3292, 1733, 1685, 1646, 1524. ^{1}H-NMR (400 MHz, $CDCl_3$): 7.34–7.16 (*m*, 10 arom. H, Bn, Phol); 7.02 (*d*, NH); 6.60 (*d*, NH); 5.25 (*d*, NH); 4.49 (*m*, CH_2, Bn); 4.38 (*m*, α-CH); 4.29 (*m*, α-CH); 4.08 (*m*, α-CH); 3.68 (*s*, Glu(O*Me*)); 3.67 (*s*, Glu(O*Me*)); 3.41 (*m*, C*H*$_2$O Phol); 2.89 (*m*, β-CH_2, Phol); 2.38 (*m*, 2 β-CH_2, Glu(OMe)); 2.06 (*m*, 2 H, 2 γ-C*H*$_2$, Glu(OMe)); 1.90 (*m*, 2 H, 2 γ-C*H*$_2$, Glu(OMe)); 1.45 (*s*, Boc). ^{13}C-NMR (150 MHz, $CDCl_3$): 173.94; 173.76; 171.58; 170.06; 165.92; 165.64; 165.14; 164.75; 163.94; 155.71; 137.91; 129.34; 128.42; 127.78; 127.73; 126.44; 73.20; 69.82; 54.06; 52.70; 51.90; 50.57; 37.41; 30.09; 28.31; 27.65; 27.58. ESI-TOF-MS: 628.30 ($[M+H]^+$; calc. 628.36).

Boc-Aib-Glu(OMe)-Glu(OMe)-Phol-Bn. Yield: 81%. M.p. 91–92°. R_{f1} 0.95, R_{f2} 0.95, R_{f3} 0.10, R_{f4} 0.95. IR (KBr): 3309, 1738, 1657, 1526. ^{1}H-NMR (400 MHz, $CDCl_3$): 7.89 (*m*, NH); 7.62 (*d*, NH); 7.37–7.12 (*m*, 10 arom. H, Bn, Phol); 6.97 (*d*, NH); 5.00 (*s*, NH, Aib); 4.54 (*m*, CH_2, Bn); 4.39 (*m*, 2 α-CH); 4.20 (*m*, α-CH); 3.72 (*s*, Glu(O*Me*)); 3.64 (*s*, Glu(O*Me*)); 3.51 (*m*, C*H*$_2$O, Phol); 3.07 (*m*, 1 H, β-CH_2, Phol); 2.79 (*m*, 1 H, β-CH_2, Phol); 2.57–2.42 (*m*, 2 H); 2.41–2.06 (*m*, 5 H); 1.94 (*m*, 1 H of γ-CH_2, Glu(OMe)); 1.48 (*s*, 1 Me, Aib); 1.44 (*s*, Boc); 1.41 (*s*, 1 Me, Aib). ^{13}C-NMR (150 MHz, $CDCl_3$): 175.61; 175.44; 173.15; 171.07; 170.57; 155.52; 138.67; 129.44; 128.23; 128.18; 127.62; 127.32; 126.07; 81.04; 73.03; 70.92; 56.76; 55.38; 53.26; 52.22; 51.51; 50.59; 37.61; 30.74; 28.25; 27.00; 26.55; 25.39; 24.00. ESI-TOF-MS: 713.34 ($[M+H]^+$; calc. 713.32).

Boc-Aib-Aib-Glu(OMe)-Glu(OMe)-Phol-Bn. Yield: 85%. M.p. 124–125°. R_{f1} 0.95, R_{f2} 0.95, R_{f3} 0.95, R_{f4} 0.95. IR (KBr): 3370, 3293, 1740, 1680, 1653, 1532. ^{1}H-NMR (400 MHz, $CDCl_3$): 7.64 (*d*, NH); 7.62 (*d*, NH); 7.36–7.13 (*m*, 10 arom. H, Bn, Phol); 6.90 (*d*, NH); 6.62 (*s*, NH, Aib); 4.99 (*s*, NH, Aib); 4.54 (*m*, CH_2, Bn); 4.35 (*m*, 2 α-CH); 4.17 (*m*, α-CH); 3.65 (*s*, Glu(O*Me*)); 3.64 (*s*, Glu(O*Me*)); 3.50 (*m*, C*H*$_2$O,

Phol); 3.06 (*m*, 1 H); 2.78 (*m*, 1 H); 2.57–2.42 (*m*, 2 H); 2.40–2.20 (*m*, 4 H); 2.15–1.91 (*m*, 2 H); 1.49 (*s*, 1 Me, Aib); 1.45 (*s*, Boc); 1.43 (*s*, 1 Me, Aib); 1.41 (*s*, 2 Me, Aib). ^{13}C-NMR (150 MHz, $CDCl_3$): 175.73; 175.09; 173.25; 171.82; 171.13; 155.83; 138.49; 129.43; 128.20; 128.08; 127.68; 127.33; 126.01; 81.10; 73.07; 71.22; 56.71; 56.63; 54.93; 53.37; 51.56; 51.43; 50.48; 37.74; 30.99; 30.80; 28.18; 27.60; 26.64; 26.49; 26.02; 23.16. ESI-TOF-MS: 798.38 ($[M+H]^+$; calc. 798.42).

Boc-Val-Aib-Aib-Glu(OMe)-Glu(OMe)-Phol-Bn. Yield: 86%. M.p. 139–140°. R_{f1} 0.95, R_{f2} 0.95, R_{f3} 0.95, R_{f4} 0.95. IR (KBr): 3288, 1740, 1651, 1534. ^{1}H-NMR (400 MHz, $CDCl_3$): 7.66 (*d*, NH); 7.58 (*d*, NH); 7.41–7.18 (*m*, 10 arom. H, Bn, Phol); 7.14 (*d*, NH); 6.99 (*d*, NH); 6.51 (*s*, NH, Aib); 4.97 (*s*, NH, Aib); 4.56 (*m*, CH_2, Bn); 4.37 (*m*, 2 α-CH); 4.13 (*m*, α-CH); 3.71 (*m*, α-CH); 3.65 (*s*, Glu(O*Me*)); 3.63 (*s*, Glu(O*Me*)); 3.51 (*m*, CH_2O, Phol); 3.10 (*m*, 1 H); 2.79 (*m*, 1 H); 2.58–2.48 (*m*, 2 H); 2.44–2.14 (*m*, 5 H); 2.12–1.95 (*m*, 2 H); 1.49 (*m*, Boc, 1 Me of Aib); 1.47 (*s*, 1 Me, Aib); 1.46 (*s*, 1 Me, Aib); 1.40 (*s*, 1 Me, Aib); 1.01 (2*d*, 2 γ-Me, Val). ^{13}C-NMR (150 MHz, $CDCl_3$): 176.25; 174.64; 173.28; 173.02; 172.28; 172.15; 171.19; 156.92; 150.19; 138.65; 129.46; 128.16; 128.04; 127.61; 127.23; 125.92; 81.25; 73.04; 71.17; 62.31; 57.00; 56.63; 55.03; 53.36; 51.53; 51.39; 50.58; 37.73; 31.03; 30.89; 29.62; 28.21; 27.45; 27.23; 26.52; 26.08; 23.26; 23.03; 18.94; 18.59. ESI-TOF-MS: 897.45 ($[M+H]^+$; calc. 897.52).

Boc-Pro-Val-Aib-Aib-Glu(OMe)-Glu(OMe)-Phol-Bn. Yield: 87%. M.p. 68–69°. R_{f1} 0.95, R_{f2} 0.95, R_{f3} 0.95, R_{f4} 0.95. IR (KBr): 3301, 1739, 1653, 1533. ^{1}H-NMR (400 MHz, $CDCl_3$): 7.71 (*s*, NH, Aib); 7.66 (*d*, NH); 7.59 (*d*, NH); 7.29–7.04 (*m*, 10 arom. H, Bn, Phol); 7.14 (*d*, NH); 6.95 (*d*, NH); 6.31 (*d*, NH); 4.48 (*m*, CH_2, Bn); 4.30 (*m*, 2 α-CH); 4.13 (*m*, α-CH); 4.05 (*m*, α-CH); 3.86 (*m*, α-CH); 3.57 (*s*, Glu(O*Me*)); 3.55 (*s*, Glu(O*Me*)); 3.51–3.41 (*m*, CH_2O of Phol, δ-CH_2 of Pro); 3.03 (*m*, 1 H, β-CH_2, Phol); 2.71 (*m*, 1 H, β-CH_2, Phol); 2.51–2.36 (*m*, 2 H); 2.35–2.12 (*m*, 7 H); 2.00–1.84 (*m*, 4 H); 1.44 (*m*, Boc); 1.42 (*s*, 2 Me, Aib); 1.37 (*s*, 2 Me, Aib); 0.92 (*d*, γ-Me, Val); 0.86 (*d*, γ-Me, Val). ^{13}C-NMR (150 MHz, $CDCl_3$): 175.28; 174.59; 173.33; 172.92; 171.54; 171.00; 155.71; 138.70; 129.51; 128.22; 128.13; 127.66; 127.27; 126.01; 81.61; 73.05; 70.95; 56.94; 56.70; 54.91; 53.22; 51.62; 51.46; 50.60; 37.66; 31.09; 30.99; 28.21; 27.75; 26.56; 26.06; 23.33. ESI-TOF-MS: 994.48 ($[M+H]^+$; calc. 994.51).

Boc-Pro-Val-Aib-Aib-Glu(OMe)-Glu(OMe)-Phol. Yield: 99%. M.p. 86–87°. R_{f1} 0.95, R_{f2} 0.95, R_{f3} 0.95, R_{f4} 0.95. IR (KBr): 3303, 1740, 1656, 1535. ^{1}H-NMR (400 MHz, $CDCl_3$): 7.94 (*d*, NH); 7.82 (*s*, NH, Aib); 7.68 (*d*, NH); 7.32–7.22 (*m*, 5 arom. H, Phol); 7.15 (*d*, NH); 7.04 (*d*, NH); 6.40 (*d*, NH); 4.31 (*m*, α-CH); 4.20 (*m*, α-CH); 4.10 (*m*, α-CH); 3.93 (*m*, α-CH); 3.72 (*m*, α-CH); 3.65 (*s*, Glu(O*Me*)); 3.64 (*s*, Glu(O*Me*)); 3.59–3.49 (*m*, 3 H); 2.96 (*m*, 2 H); 2.60–2.46 (*m*, 2 H); 2.42–2.10 (*m*, 7 H); 2.10–1.91 (*m*, 4 H); 1.60 (*s*, 6 H); 1.51 (*m*, 12 H); 1.46 (*s*, 6 H); 0.99 (*d*, γ-Me, Val); 0.94 (*d*, γ-Me, Val). ^{13}C-NMR (150 MHz, $CDCl_3$): 177.42; 175.32; 173.73; 173.22; 172.95; 172.51; 171.56; 171.31; 156.04; 138.89; 129.64; 128.15; 125.98; 94.99; 81.92; 63.43; 61.84; 60.48; 57.04; 56.95; 55.59; 53.96; 53.32; 51.58; 51.43; 47.53; 36.82; 31.13; 31.11; 30.06; 28.86; 28.38; 28.31; 27.83; 27.49; 26.96; 26.53; 26.02; 24.87; 23.08; 22.94; 17.07; 17.67. ESI-TOF-MS: 904.45 ($[M+H]^+$; calc. 904.51).

Z-Dab(Tfa)-Phol-Bn. Yield: 69%. M.p. 135–136°. R_{f1} 0.95, R_{f2} 0.95, R_{f3} 0.50, R_{f4} 0.75. IR (KBr): 3304, 1698, 1645, 1532. ^{1}H-NMR (400 MHz, (D_6)DMSO): 9.31 (*m*, ε-NH, Dab); 7.87 (*d*, J=8.4, NH, Dab); 7.41 (*d*, J=8.0, NH, Phol); 7.39–7.06 (*m*, 15 arom. H, Z, Bn, Phol); 5.01 (*m*, CH_2, Z); 4.44 (*m*, CH_2, Bn); 4.12–4.05 (*m*, α-CH); 4.04–3.96 (*m*, α-CH); 3.38–3.32 (*m*, 2 H); 3.21–3.09 (*m*, CH_2O, Phol); 2.84–2.77 (*m*, 1 H); 2.75–2.64 (*m*, 1 H); 1.85–1.72 (*m*, 1 H); 1.70–1.57 (*m*, 1 H). ^{13}C-NMR (150 MHz, $CDCl_3$): 170.14; 157.74; 157.50; 156.73; 137.65; 137.53; 135.83; 129.31; 128.64; 128.53; 128.44; 128.13; 127.99; 126.63; 73.33; 69.39; 67.49; 52.28; 50.92; 37.41; 35.93; 32.94; 22.86. ESI-TOF-MS: 572.21 ($[M+H]^+$; calc. 572.23).

Boc-Glu(OMe)-Dab(Tfa)-Phol-Bn. Yield: 70%. M.p. 146–147°. R_{f1} 0.95, R_{f2} 0.95, R_{f3} 0.40, R_{f4} 0.35. IR (KBr): 3304, 1701, 1638, 1552. ^{1}H-NMR (400 MHz, $CDCl_3$): 7.82 (*m*, ε-NH, Dab); 7.35–7.05 (*m*, 10 arom. H, Phol, Bn); 6.84 (*d*, J=7.6, NH, Phol); 6.21 (*d*, J=8.4, NH, Dab); 5.11 (br. *d*, J=4.8, NH, Glu); 4.46–4.39 (*m*, CH_2, Bn); 4.29–4.14 (*m*, 2 α-CH); 4.03–3.95 (*m*, α-CH); 3.63 (*s*, Glu(O*Me*)); 3.68–3.56 (*m*, 1 H); 3.37–3.28 (*m*, CH_2O, Phol); 3.03–2.90 (*m*, 1 H); 2.86–2.78 (*m*, 2 H); 2.45–2.25 (*m*, 2 H); 2.05–1.94 (*m*, 1 H); 1.92–1.79 (*m*, 2 H); 1.71–1.59 (*m*, 1 H); 1.37 (*s*, Boc). ^{13}C-NMR (150 MHz, $CDCl_3$): 173.60; 172.70; 169.98; 157.75; 157.52; 155.87; 137.70; 129.28; 128.49; 127.92; 126.56; 118.84; 116.93; 115.02; 113.12; 80.47; 73.25; 69.52; 54.33; 51.94; 50.96; 50.80; 37.33; 35.88; 32.59; 30.28; 28.29; 28.24; 27.33. ESI-TOF-MS: 681.29 ($[M+H]^+$; calc. 681.39).

Boc-Aib-Glu(OMe)-Dab(Tfa)-Phol-Bn. Yield: 85%. M.p. 106–107°. R_{f1} 0.95, R_{f2} 0.95, R_{f3} 0.35, R_{f4} 0.30. IR (KBr): 3304, 1720, 1661, 1639, 1527. ^{1}H-NMR (400 MHz, $CDCl_3$): 8.01 (br. *d*, *J* = 4.0, NH); 7.87 (*m*, ε-NH, Dab); 7.76 (*d*, *J* = 8.0, NH); 7.38–7.10 (*m*, 10 arom. H, Phol, Bn, 2 NH); 5.07 (*s*, NH, Aib); 4.56 (*m*, CH_2, Bn); 4.42–4.36 (*m*, α-CH); 4.35–4.28 (*m*, α-CH); 4.20–4.13 (*m*, α-CH); 3.73 (*s*, Glu(O*Me*)); 3.58–3.49 (*m*, CH_2O, Phol); 3.39–3.29 (*m*, 1 H); 3.12–3.07 (*m*, 1 H); 3.05–2.98 (*m*, 1 H); 2.76–2.66 (*m*, 1 H); 2.58–2.42 (*m*, 2 H); 2.20–2.09 (*m*, 2 H); 1.92–1.84 (*m*, 2 H); 1.53 (*s*, β-Me, Aib); 1.45 (*s*, Boc); 1.41 (*s*, β-Me, Aib). ^{13}C-NMR (150 MHz, $CDCl_3$): 175.88; 171.10; 171.08; 157.42; 157.17; 155.74; 138.56; 138.51; 129.59; 129.51; 129.28; 128.55; 128.52; 128.28; 128.20; 128.14; 128.02; 127.64; 127.43; 126.21; 81.25; 73.35; 73.09; 71.10; 69.58; 63.47; 56.72; 55.54; 52.30; 51.87; 50.76; 37.88; 37.47; 36.59; 36.01; 32.92; 30.75; 30.51; 30.36; 29.41; 29.02; 28.29; 28.22; 27.11; 25.12; 25.00; 23.82; 23.39. ESI-TOF-MS: 766.32 ($[M+H]^+$; calc. 766.33).

Boc-Aib-Aib-Glu(OMe)-Dab(Tfa)-Phol-Bn (**7**). Yield: 65%. M.p. 128–129°. R_{f1} 0.95, R_{f2} 0.95, R_{f3} 0.30, R_{f4} 0.20. IR (KBr): 3301, 1724, 1661, 1533. ^{1}H-NMR (400 MHz, $CDCl_3$): 8.04 (*m*, ε-NH, Dab); 7.72 (*d*, *J* = 6.0, NH); 7.68 (*d*, *J* = 8.0, NH); 7.38–7.10 (*m*, 10 arom. H, Phol, Bn); 7.03 (*d*, *J* = 8.8, NH); 6.72 (*s*, NH, Aib); 5.13 (*s*, NH, Aib); 4.58–4.51 (*m*, CH_2, Bn); 4.43–4.28 (*m*, 2 α-CH); 4.21–4.10 (*m*, α-CH); 3.64 (*s*, Glu(O*Me*)); 3.53–3.49 (*m*, 1 H); 3.36–3.23 (*m*, CH_2O, Phol); 3.05–2.98 (*m*, 1 H); 3.09–3.01 (*m*, 1 H); 2.79–2.69 (*m*, 1 H); 2.58–2.42 (*m*, 2 H); 2.39–2.27 (*m*, 1 H); 2.14–1.98 (*m*, 2 H); 1.96–1.88 (*m*, 1 H); 1.51 (*s*, β-Me, Aib); 1.44 (*s*, β-Me Aib, Boc); 1.41 (*s*, β-Me, Aib); 1.26 (*s*, β-Me, Aib). ^{13}C-NMR (150 MHz, $CDCl_3$): 175.51; 175.04; 171.72; 171.41; 157.38; 157.14; 155.78; 138.41; 138.38; 129.44; 128.22; 128.10; 127.65; 127.38; 126.15; 81.52; 73.07; 70.94; 56.84; 56.68; 54.80; 51.64; 50.77; 37.76; 36.54; 30.94; 30.24; 28.17; 27.64; 26.74; 25.78; 23.21. ESI-TOF-MS: 851.40 ($[M+H]^+$; calc. 851.41).

Boc-Val-Aib-Aib-Glu(OMe)-Dab(Tfa)-Phol-Bn. Yield: 87%. M.p. 158–159°. R_{f1} 0.95, R_{f2} 0.95, R_{f3} 0.30, R_{f4} 0.25. IR (KBr): 3294, 1725, 1652, 1535. ^{1}H-NMR (400 MHz, $CDCl_3$): 7.99 (*m*, ε-NH, Dab); 7.70–7.62 (*m*, 2 NH); 7.52 (*s*, NH, Aib); 7.38–7.13 (*m*, 10 arom. H, Phol, Bn); 7.07 (*d*, *J* = 8.8, NH); 6.54 (*s*, NH, Aib); 4.98 (br. *d*, *J* = 2.6, NH); 4.59–4.52 (*m*, CH_2, Bn); 4.46–4.25 (*m*, 2 α-CH); 4.17–4.07 (*m*, α-CH); 3.75–3.68 (*m*, α-CH); 3.65 (*s*, Glu(O*Me*)); 3.56–3.46 (*m*, CH_2O, Phol); 3.36–3.21 (*m*, 2 H); 3.13–3.03 (*m*, 1 H); 2.79–2.69 (*m*, 1 H); 2.57–2.48 (*m*, 2 H); 2.42–2.29 (*m*, 1 H); 2.22–2.13 (*m*, 1 H); 2.12–1.88 (*m*, 3 H); 1.52 (*s*, β-Me, Aib); 1.50–1.47 (br. *s*, Boc); 1.46 (*s*, β-Me, Aib); 1.41 (*s*, β-Me, Aib); 1.03–0.97 (*m*, 2 γ-Me, Val). ^{13}C-NMR (150 MHz, $CDCl_3$): 176.14; 174.63; 173.08; 171.95; 171.54; 157.14; 156.86 138.57; 129.51; 129.27; 128.46; 128.22; 128.09; 127.94; 127.63; 127.32; 126.10; 81.71; 73.29; 73.07; 70.97; 69.55; 62.17; 57.12; 56.62; 54.83; 51.72; 51.62; 50.85; 37.76; 36.67; 31.02; 30.30; 29.66; 28.23; 27.48; 25.88; 23.33; 23.25; 19.02; 18.39. ESI-TOF-MS: 950.43 ($[M+H]^+$; calc. 950.41).

Boc-Pro-Val-Aib-Aib-Glu(OMe)-Dab(Tfa)-Phol-Bn. Yield: 71%. M.p. 84–85°. R_{f1} 0.95, R_{f2} 0.95, R_{f3} 0.25, R_{f4} 0.25. IR (KBr): 3303, 1723, 1657, 1533. ^{1}H-NMR (400 MHz, $CDCl_3$): 8.03 (*m*, ε-NH, Dab); 7.81 (*s*, NH, Aib); 7.76–7.68 (*m*, 2 NH); 7.35–7.16 (*m*, 10 arom. H, Phol, Bn); 7.14 (*d*, *J* = 7.2, NH); 7.10 (*d*, *J* = 8.8, NH); 6.38 (*d*, *J* = 5.2, NH); 4.59–4.52 (*m*, CH_2, Bn); 4.41–4.31 (*m*, 2 α-CH); 4.24–4.18 (*m*, α-CH); 4.17–4.08 (*m*, α-CH); 3.96–3.89 (*m*, α-CH); 3.64 (*s*, Glu(O*Me*)); 3.60–3.46 (*m*, CH_2O, Phol, δ-CH_2, Pro); 3.55–3.20 (*m*, 2 H); 3.15–3.03 (*m*, 1 H); 2.79–2.69 (*m*, 1 H); 2.56–2.45 (*m*, 2 H); 2.43–2.31 (*m*, 2 H); 2.27–2.20 (*m*, 1 H); 2.08–1.88 (*m*, 6 H); 1.57 (*s*, 2 β-Me, Aib); 1.52 (*s*, Boc); 1.45 (*s*, β-Me, Aib); 1.43 (*s*, β-Me, Aib); 0.99 (*d*, *J* = 6.8, γ-Me, Val); 0.93 (*d*, *J* = 6.8, γ-Me, Val). ^{13}C-NMR (150 MHz, $CDCl_3$): 176.38; 175.32; 173.69; 173.10; 172.15; 171.48; 171.39; 157.33; 157.08; 156.01; 138.67; 129.55; 128.20; 128.05; 127.64; 127.28; 126.03; 81.92; 73.05; 71.04; 61.81; 60.40; 57.00; 54.81; 51.81; 51.56; 50.72; 47.51; 37.82; 36.64; 31.10; 30.36; 30.05; 28.83; 28.29; 27.55; 26.94; 25.90; 24.84; 23.20; 22.97; 19.08; 17.61. ESI-TOF-MS: 1047.51 ($[M+H]^+$; calc. 1047.58).

Boc-Pro-Val-Aib-Aib-Glu(OMe)-Dab(Tfa)-Phol. Yield: 99%. M.p. 95–96°. R_{f1} 0.95, R_{f2} 0.95, R_{f3} 0.20, R_{f4} 0.10. IR (KBr): 3302, 1724, 1656, 1537. ^{1}H-NMR (400 MHz, $CDCl_3$): 7.88–7.81 (*m*, 2 NH); 7.77 (*s*, NH, Aib); 7.65 (*d*, *J* = 7.6, NH); 7.26–7.13 (*m*, 5 arom. H, Phol); 7.09 (*d*, *J* = 7.2, NH); 7.04 (*d*, *J* = 8.8, NH); 6.32 (br. *d*, *J* = 4.4, NH); 4.26–4.18 (*m*, α-CH); 4.17–4.06 (*m*, 2 α-CH); 4.04–3.95 (*m*, α-CH); 3.89–3.82 (*m*, α-CH); 3.71–3.66 (*m*, 1 H of δ-CH_2 Pro); 3.58 (*s*, Glu(O*Me*)); 3.55–3.44 (*m*, CH_2OH, Phol, 1 H of δ-CH_2 Pro); 3.39–3.29 (*m*, 1 H); 3.17–3.04 (*m*, 1 H); 2.89–2.82 (*m*, 1 H of β-CH_2 Phol); 2.80–2.73 (*m*, 1 H of β-CH_2 Phol); 2.52–2.40 (*m*, 2 H); 2.36–2.21 (*m*, 2 H); 2.20–2.40 (*m*, 2 H); 1.98–1.83 (*m*, 5 H); 1.55 (*s*, 2 β-Me, Aib); 1.45 (*s*, Boc); 1.40 (*s*, β-Me, Aib); 1.39 (*s*, β-Me, Aib); 0.93 (*d*, *J* = 6.8, γ-Me, Val); 0.88 (*d*, *J* = 6.8, γ-Me, Val). ^{13}C-NMR (150 MHz, $CDCl_3$): 177.46; 175.64; 173.83; 173.07;

172.56; 171.79; 171.69; 157.44; 157.19; 156.07; 138.68; 129.65; 128.14; 126.14; 116.92; 115.01; 81.96; 63.76; 61.85; 60.58; 57.00; 56.97; 55.56; 53.29; 52.26; 51.66; 47.54; 36.88; 36.71; 30.98; 30.27; 30.08; 28.88; 28.32; 27.44; 26.95; 25.82; 24.86; 23.25; 22.89; 19.06; 17.74. ESI-TOF-MS: 957.45 ($[M+H]^+$; calc. 957.51).

Tfa-Aib-Pro-Aib-Ala-Aib-OBn. Yield: 99%. M.p. 221–222°. R_{f1} 0.60, R_{f2} 0.95, R_{f3} 0.25. IR (film on KBr): 3334, 1739, 1707, 1664, 1627, 1528. ^{1}H-NMR (400 MHz, $CDCl_3$): 8.89 (*s*, NH); 7.51–7.49 (*d*, NH); 7.44 (*s*, NH); 7.33 (*m*, 5 arom. H, Bn); 7.14 (*s*, NH); 5.11–5.10 (*m*, CH_2, Bn); 4.28 (*m*, α-CH); 4.20 (*m*, α-CH); 3.93 (*m*, 1 H); 3.22–3.20 (*m*, 1 H); 2.38 (*m*, 1 H); 1.91–1.89 (*m*, 1 H); 1.73 (*m*, 2 H); 1.56 (*s*, 3 H); 1.54 (*s*, 6 H); 1.53 (*s*, 3 H); 1.52 (*s*, 3 H); 1.45 (*s*, 3 H); 1.40–1.68 (*d*, 3 H). ^{13}C-NMR (150 MHz, $CDCl_3$): 174.81; 174.20; 172.98; 172.30; 172.06; 157.40; 157.14; 136.13; 128.31; 127.70; 121.07; 118.52; 116.61; 114.70; 112.80; 66.42; 64.74; 57.79; 57.00; 55.91; 49.72; 48.82; 28.68; 27.25; 26.33; 25.47; 25.14; 24.33; 23.72; 23.28; 17.05. ESI-TOF-MS: 628.26 ($[M+H]^+$; calc. 628.29).

Z-Dab(Tfa)-Aib-Gly-Leu-Aib-O^{t}Bu. Yield: 82%. M.p. 91–92°. R_{f1} 0.50, R_{f2} 0.90, R_{f3} 0.25. IR (KBr): 3374, 1716, 1660, 1538. ^{1}H-NMR (400 MHz, $CDCl_3$): 7.90 (*m*, NH); 7.47 (*m*, NH); 7.39–7.28 (*m*, 5 arom. H, Z); 6.98 (*m*, NH); 7.06 (*m*, NH); 6.91 (*s*, NH); 6.44 (*d*, NH); 5.10 (2*d*, CH_2, Z); 4.35 (*m*, α-CH, Leu); 4.08–3.93 (*m*, α-CH Gly, α-CH of Dab); 3.71–3.63 (*m*, α-CH of Gly); 3.62–3.50 (*m*, 1 H); 3.41–3.28 (*m*, 1 H); 2.23–2.11 (*m*, 1 H); 2.01–1.89 (*m*, 1 H); 1.75–1.59 (*m*, 3 H); 1.64 (*s*, β-Me, Aib); 1.45 (*s*, β-Me, Aib); 1.42 (*s*, ^{t}BuO); 1.38 (*s*, β-Me, Aib); 0.91 (*d*, J=5.6, 1 δ-Me, Leu); 0.86 (*d*, J=5.6, 1 δ-Me, Leu). ^{13}C-NMR (150 MHz, $CDCl_3$): 175.18; 173.47; 172.46; 172.42; 172.28; 170.69; 158.02; 157.73; 157.12; 136.17; 128.60; 128.34; 127.77; 116.89; 114.99; 81.33; 67.32; 57.00; 56.70; 53.33; 52.85; 43.45; 39.88; 36.60; 30.08; 27.78; 24.84; 24.77; 24.65; 23.01; 21.19. ESI-TOF-MS: 745.43 ($[M+H]^+$; calc. 745.34).

Z-Aib-Dab(Tfa)-Aib-Gly-Leu-Aib-O^{t}Bu (**6**). Yield: 86%. M.p. 200–201°. R_{f1} 0.50, R_{f2} 0.80, R_{f3} 0.25. IR (KBr): 3365, 3309, 1705, 1650, 1538. ^{1}H-NMR (400 MHz, $CDCl_3$): 7.97 (*m*, NH); 7.63 (*d*, J=7.4, NH); 7.58 (*s*, NH); 7.46 (*d*, J=7.9, NH); 7.39–7.28 (*m*, 5 arom. H, Z); 7.16 (*m*, NH); 6.79 (*s*, NH); 5.30 (*s*, NH); 5.06 (*m*, CH_2, Z); 4.42–4.36 (*m*, α-CH, Leu); 4.26–4.14 (*m*, α-CH of Gly, α-CH of Dab); 3.70–3.64 (*m*, α-CH Gly); 3.49–3.40 (*m*, 1 H); 3.38–3.30 (*m*, 1 H); 2.17–2.01 (*m*, 2 H); 1.82–1.63 (*m*, 3 H); 1.59 (*s*, β-Me, Aib); 1.52 (*s*, β-Me, Aib); 1.50 (*s*, β-Me, Aib); 1.48 (*s*, β-Me, Aib); 1.46 (*s*, β-Me, Aib); 1.44 (*s*, β-Me, Aib); 1.43 (*s*, ^{t}BuO); 0.93 (*d*, J=6.3, 1 δ-Me, Leu); 0.90 (*d*, J=6.3, 1 δ-Me, Leu). ^{13}C-NMR (150 MHz, $CDCl_3$): 175.53; 174.60; 172.00; 171.87; 170.47; 157.26; 155.84; 135.74; 134.08; 128.64; 128.46; 127.91; 97.05; 94.98; 81.30; 67.37; 57.26; 57.08; 52.05; 51.84; 43.21; 39.72; 37.00; 29.07; 27.79; 27.75; 26.10; 25.63; 25.28; 24.79; 24.61; 24.45; 23.91; 23.03; 21.65. ESI-TOF-MS: 830.43 ($[M+H]^+$; calc. 830.40).

Z-Glu(OMe)-Aib-Dab(Tfa)-Aib-Gly-Leu-Aib-O^{t}Bu. Yield: 80%. M.p. 88–89°. R_{f1} 0.45, R_{f2} 0.85, R_{f3} 0.20. IR (KBr): 3396, 1722, 1658, 1533. ^{1}H-NMR (400 MHz, $CDCl_3$): 8.07 (*m*, NH); 7.57 (*d*, J=7.0, NH); 7.55 (*s*, NH); 7.49 (*d*, J=7.6, NH); 7.41–7.31 (*m*, 5 arom. H, Z); 6.98 (*s*, NH); 6.68 (*s*, NH); 6.26 (*d*, NH); 5.09 (*m*, CH_2, Z); 4.42–4.31 (*m*, α-CH, Leu); 4.09–4.03 (*m*, α-CH, Gly); 3.99–3.89 (*m*, α-CH of Dab, α-CH of Glu(OMe)); 3.72 (*s*, Glu(O*Me*)); 3.69–3.61 (*m*, α-CH, Gly); 3.54–3.37 (*m*, 2 H); 2.63–2.55 (*m*, 1 H); 2.52–2.43 (*m*, 1 H); 2.20–1.95 (*m*, 4 H); 1.80–1.67 (*m*, 3 H); 1.59 (*s*, β-Me, Aib); 1.62 (*s*, β-Me, Aib); 1.47 (*s*, 2 β-Me, Aib); 1.45 (*s*, β-Me, Aib); 1.41 (*s*, ^{t}BuO); 1.39 (*s*, β-Me, Aib); 0.92 (*d*, J=6.3, 1 δ-Me, Leu); 0.89 (*d*, J=6.3, 1 δ-Me, Leu). ^{13}C-NMR (150 MHz, $CDCl_3$): 175.60; 175.45; 173.95; 173.36; 172.53; 172.40; 172.04; 170.51; 157.78; 157.53; 157.47; 135.81; 128.69; 128.46; 127.65; 116.83; 114.92; 81.15; 67.53; 57.24; 56.93; 56.73; 56.42; 52.97; 52.33; 52.12; 43.48; 39.46; 36.97; 30.39; 29.80; 27.79; 27.77; 27.74; 25.88; 25.16; 24.87; 24.81; 24.52; 24.43; 24.36; 23.00; 21.43. ESI-TOF-MS: 973.51 ($[M+H]^+$; calc. 973.51).

Z-Ala-Glu(OMe)-Aib-Dab(Tfa)-Aib-Gly-Leu-Aib-O^{t}Bu. Yield: 77%. M.p. 94–95°. R_{f1} 0.45, R_{f2} 0.85, R_{f3} 0.15. HPLC: t_R 10.68 min (flow rate, 1 ml/min; gradient, 40–90% *B* in 25 min; *C$_4$ Vydac* column). IR (KBr): 3370, 1722, 1659, 1533. ^{1}H-NMR (400 MHz, $CDCl_3$): 8.02 (*m*, NH, Glu(OMe)); 7.67 (*m*, ε-NH, Dab); 7.64 (*s*, NH, Aib); 7.52 (*d*, J=7.7, NH, Leu); 7.46 (*d*, J=6.6, α-NH, Dab); 7.40 (*s*, NH, Aib); 7.37–7.29 (*m*, 5 arom. H, Z); 7.06 (*s*, NH, Aib); 5.69 (*d*, NH, Ala); 5.14 (*m*, CH_2, Z); 4.40–4.30 (*m*, α-CH, Leu); 4.27–4.17 (*m*, α-CH, Dab); 4.08–3.91 (*m*, α-CH of Ala, α-CH of Glu(OMe), 1 H of α-CH_2, Gly); 3.78–3.72 (*m*, 1 H of α-CH_2, Gly); 3.69 (*s*, Glu(O*Me*)); 3.52–3.37 (*m*, β-CH_2, Dab); 2.59–2.45 (*m*, β-CH_2, Glu); 2.20–2.10 (*m*, 1 H of γ-CH_2, Dab); 2.09–1.98 (*m*, 1 H of γ-CH_2 of Dab: γ-CH_2 of Glu(OMe)); 1.82–1.63 (*m*, β-CH_2 and γ-CH, Leu); 1.51 (*s*, β-Me, Aib); 1.50 (*s*, β-Me, Aib); 1.49 (*s*, β-Me, Aib); 1.48 (*m*, β-Me, Aib); 1.43 (*m*, 2 β-Me of Aib, β-Me of Ala); 1.39 (*s*, ^{t}BuO); 0.91 (*d*, J=5.6, 1 δ-Me, Leu); 0.88 (*d*, J=7.0, 1 δ-Me, Leu). ^{13}C-NMR (150 MHz, $CDCl_3$): 175.63; 175.55; 175.04; 173.50; 172.70; 172.00; 171.87; 171.77; 170.13; 157.26; 157.08; 135.94; 128.63; 128.44; 127.79; 80.85; 67.53; 57.21; 57.14;

56.55; 56.29; 56.02; 52.89; 52.80; 52.70; 52.33; 52.17; 43.63; 39.35; 36.83; 30.57; 30.16; 27.82; 27.72; 26.74; 26.69; 25.10; 24.92; 24.59; 24.34; 23.35; 23.29; 23.08; 22.89; 21.46; 20.89; 17.37; 17.32. ESI-TOF-MS: 1044.52 ($[M+H]^+$; calc. 1044.56).

Z-Ala-Glu(OMe)-Aib-Dab(Tfa)-Aib-Gly-Leu-Aib-Pro-Val-Aib-Aib-Glu(OMe)-Glu(OMe)-Phol. Yield: 30%. IR (film on KBr): 3321, 1737, 1656, 1533. ^{1}H-NMR (600 MHz, $CDCl_3$): 8.33 (*m*, 1 H); 7.94 (*m*, 1 H); 7.92–7.91 (*m*, 2 H); 7.87–7.85 (*m*, 2 H); 7.80 (*m*, 1 H); 7.73 (*m*, 1 H); 7.69–7.67 (*m*, 2 H); 7.60–7.56 (*m*, 4 H); 7.49–7.47 (*m*, 2 H); 7.40 (*m*, 2 H); 7.36–7.34 (*m*, 7 H); 7.23 (*s*, 1 H); 7.22 (*s*, 1 H); 7.19–7.14 (*m*, 2 H); 5.14 (*m*, 2 H); 4.43–4.16 (*m*, 5 H); 4.09–4.01 (*m*, 4 H); 3.89–3.88 (*m*, 1 H); 3.76–3.74 (*m*, 1 H); 3.72 (*m*, 1 H); 3.69–3.67 (*m*, 4 H); 3.66 (*m*, 1 H); 3.64 (*m*, 2 H); 3.634 (*m*, 1 H); 3.627 (*m*, 3 H); 3.60 (*m*, 3 H); 3.56–3.51 (*m*, 3 H); 2.95–2.77 (*m*, 3 H); 2.75–2.65 (*m*, 1 H); 2.51 (*m*, 4 H); 2.38–2.36 (*m*, 2 H); 2.35–2.26 (*m*, 4 H); 2.25–2.15 (*m*, 6 H); 2.12–1.98 (*m*, 9 H); 1.95–1.66 (*m*, 21 H); 1.64 (*m*, 1 H); 1.61 (*s*, 3 H); 1.57 (*s*, 3 H); 1.55 (*s*, 6 H); 1.53 (*s*, 6 H); 1.52 (*s*, 3 H); 1.50 (*s*, 3 H); 1.49 (*s*, 3 H); 1.48 (*s*, 6 H); 1.45 (*s*, 6 H); 1.44 (*s*, 3 H); 1.41 (*s*, 3 H); 1.03 (*m*, 3 H); 0.97–0.92 (*m*, 6 H); 0.90–0.89 (*m*, 3 H). ^{13}C-NMR (150 MHz, $CDCl_3$): 177.60; 177.39; 176.35; 175.81; 174.58; 174.11; 174.06; 166.78; 159.85; 137.15; 136.81; 135.80; 135.42; 129.62; 128.70; 128.59; 128.20; 123.23; 122.89; 112.98; 68.10; 63.51; 63.41; 61.27; 56.40; 51.72; 49.43; 49.17; 44.57; 44.32; 43.11; 33.84; 33.16; 30.98; 30.91; 30.85; 30.19; 29.66; 29.59; 29.28; 29.25; 27.03; 26.34; 26.31; 26.26; 25.65; 18.11; 17.98; 17.76; 17.43; 17.29. ESI-TOF-MS: 1774.81 ($[M+H]^+$); 887.40 ($[M+2\,H]^{2+}$; calc. 887.40).

Z-Ala-Glu(OMe)-Aib-Val-Aib-Gly-Leu-Aib-Pro-Val-Aib-Aib-Glu(OMe)-Dab(Tfa)-Phol. Yield: 30%. IR (film on KBr): 3321, 1727, 1655, 1533. ^{1}H-NMR (600 MHz, $CDCl_3$): 8.33 (*m*, 1 H); 7.93–7.91 (*m*, 5 H); 7.82–7.80 (*m*, 1 H); 7.76 (*t*, 1 H); 7.72 (*s*, 1 H); 7.58 (*s*, 1 H); 7.56–7.55 (*d*, 1 H); 7.52–7.51 (*d*, 1 H); 7.42–7.40 (*m*, 2 H); 7.36–7.34 (*m*, 7 H); 7.22–7.19 (*m*, 5 H); 7.16–7.15 (*m*, 2 H); 5.15–5.13 (*m*, 2 H); 4.41–4.37 (*m*, 1 H); 4.31–4.26 (*m*, 3 H); 4.06–3.96 (*m*, 6 H); 3.78–3.76 (*m*, 2 H); 3.72–3.70 (*m*, 2 H); 3.68–3.65 (*m*, 7 H); 3.64–3.59 (*m*, 6 H); 3.55–3.54 (*m*, 1 H); 3.39–3.37 (*m*, 1 H); 3.21–3.16 (*m*, 1 H); 2.82–2.79 (*m*, 2 H); 2.68–2.64 (*m*, 1 H); 2.50 (*m*, 5 H); 2.35–2.17 (*m*, 21 H); 2.11–2.06 (*m*, 5 H); 1.97–1.93 (*m*, 6 H); 1.80–1.79 (*m*, 2 H); 1.61 (*s*, 3 H); 1.56 (*s*, 3 H); 1.54 (*s*, 6 H); 1.53 (*s*, 3 H); 1.50 (*s*, 6 H); 1.49 (*s*, 3 H); 1.48 (*s*, 3 H); 1.47 (*s*, 6 H); 1.45 (*s*, 6 H); 1.44 (*s*, 3 H); 1.42 (*s*, 3 H); 1.39 (*m*, 5 H); 1.07–0.88 (*m*, 12 H). ^{13}C-NMR (150 MHz, $CDCl_3$): 177.53; 177.41; 176.34; 176.18; 174.69; 173.49; 173.17; 172.50; 170.42; 157.27; 136.28; 129.60; 128.75; 128.67; 128.45; 128.34; 128.16; 128.11; 127.71; 127.60; 126.24; 67.32; 64.14; 63.50; 56.73; 56.42; 56.21; 53.46; 53.19; 52.93; 52.43; 51.60; 49.24; 44.46; 40.13; 39.82; 36.95; 36.49; 30.72; 30.62; 29.29; 29.09; 27.83; 27.03; 26.99; 26.21; 25.56; 25.16; 24.62; 24.40; 23.38; 23.12; 23.03; 22.62; 22.55; 21.11; 20.11; 19.58; 19.12; 18.97; 17.35; 17.24. ESI-TOF-MS: 1730.95 ($[M+H]^+$); 865.93 ($[M+2\,H]^{2+}$; calc. 866.01).

Tfa-Aib-Pro-Aib-Ala-Aib-Ala-Glu(OMe)-Aib-Val-Aib-Gly-Leu-Aib-Pro-Val-Aib-Aib-Glu(OMe)-Glu(OMe)-Phol (**N$^{\alpha}$TfaAlm′**; **2**). Yield: 51%. HPLC: t_R 22.58 min (flow rate: 1 ml/min; gradient: 60–100% *B* in 30 min; *C_{18} Agilent Zorbax* column). IR (film on KBr): 3328, 1740, 1666, 1535. ^{1}H-NMR (600 MHz, $CDCl_3$): 9.92 (*s*, 1 H); 8.25 (*s*, 1 H); 8.08 (*m*, 1 H); 7.98 (*s*, 1 H); 7.93 (*m*, 1 H); 7.88–7.85 (*m*, 3 H); 7.79 (*s*, 1 H); 7.65–7.50 (*m*, 5 H); 7.39–7.38 (*d*, 1 H); 7.30–7.28 (*m*, 2 H); 7.24–7.21 (*m*, 2 H); 7.16–7.14 (*m*, 1 H); 7.045 (*s*, 1 H); 4.41 (*m*, 1 H); 4.30–4.28 (*m*, 1 H); 4.19 (*m*, 2 H); 4.14–4.13 (*m*, 1 H); 4.07–3.97 (*m*, 5 H); 3.88 (*m*, 1 H); 3.81 (*m*, 2 H); 3.66 (*m*, 2 H); 3.64 (*s*, 3 H); 3.63 (*s*, 3 H); 3.61 (*s*, 3 H); 3.55–3.49 (*m*, 2 H); 3.29 (*m*, 1 H); 2.82–2.81 (*d*, 2 H); 2.73–2.66 (*m*, 2 H); 2.56–2.52 (*m*, 2 H); 2.40 (*m*, 10 H); 2.32–2.06 (*m*, 12 H); 1.96–1.89 (*m*, 4 H); 1.80–1.72 (*m*, 3 H); 1.62–1.60 (*m*, 10 H); 1.55 (*m*, 15 H); 1.53 (*m*, 9 H); 1.51 (*s*, 3 H); 1.50 (*m*, 6 H); 1.49 (*s*, 3 H); 1.57 (*m*, 6 H); 1.12–1.11 (*d*, 3 H); 1.08–1.07 (*d*, 3 H); 1.00–0.99 (*d*, 3 H); 0.94–0.91 (*m*, 9 H). ^{13}C-NMR (150 MHz, $CDCl_3$): 177.53; 177.35; 176.60; 176.51; 176.23; 176.18; 175.31; 174.82; 174.08; 173.97; 173.87; 173.69; 173.31; 173.27; 173.11; 173.08; 172.89; 170.94; 157.88; 157.63; 138.54; 129.52; 128.10; 126.07; 64.71; 63.97; 63.53; 63.39; 57.87; 56.75; 56.72; 56.41; 56.35; 56.12; 56.02; 55.08; 53.18; 52.82; 52.68; 52.44; 51.56; 51.47; 51.31; 49.36; 49.30; 44.52; 40.41; 37.21; 30.78; 30.74; 30.72; 29.67; 29.22; 29.09; 28.99; 28.92; 26.97; 26.94; 26.87; 26.47; 26.38; 26.21; 26.01; 25.92; 25.57; 25.24; 24.53; 23.50; 23.30; 22.99; 22.84; 22.67; 22.58; 22.47; 21.21; 20.55; 20.14; 19.26; 18.80; 16.76; 16.60. ESI-TOF-MS: 2062.12 ($[M+H]^+$; calc. 2062.10); 1031.54 ($[M+2\,H]^{2+}$).

Ac-Aib-Pro-Aib-Ala-Aib-Ala-Glu(OMe)-Aib-Dab(Tfa)-Aib-Gly-Leu-Aib-Pro-Val-Aib-Aib-Glu(OMe)-Glu(OMe)-Phol (**DabTfa9Alm′**; **3**). Yield: 52%. HPLC: t_R 16.52 min (flow rate, 1 ml/min; gradient, 40–90% *B* in 30 min; *C_4 Vydac* column). IR (film on KBr): 3317, 1738, 1655, 1535. ^{1}H-NMR

(600 MHz, CD_3OH): 8.30–8.27 (*m*, 3 NH, Aib[8], Aib[10], Gly[11]); 8.18 (*s*, NH, Aib[13]); 8.09–8.08 (*d*, NH, Leu[12]); 8.05–8.04 (*d*, NH, Glu(OMe)[7]); 7.98–7.97 (*d*, NH, Ala[6]); 7.96 (*s*, NH, Aib[5]); 7.90–7.87 (*m*, 3 NH, Aib[1], Glu(OMe)[18], Glu(OMe)[19]); 7.80 (*s*, NH, Aib[17]); 7.78–7.77 (*d*, NH, Dab(Tfa)[9]); 7.62 (*s*, NH, Aib[3]); 7.59–7.58 (*m*, 2 NH, Val[15], Ala[4]); 7.57 (*s*, NH, Aib[16]); 7.34–7.31 (*m*, NH, H_p Phol); 7.25–7.22 (*t*, 2 H_m Phol); 7.17–7.15 (*t*, 2 H_o Phol); 4.48–4.40 (*m*, α-CH Leu[12]); 4.40–4.38 (*m*, α-CH Pro[14]); 4.28–4.25 (*m*, α-CH Pro[2]); 4.21–4.14 (*m*, 2 α-CH Glu(OMe)[19], Phol); 4.10–4.09 (*m*, α-CH Ala[6]); 4.06–4.03 (*m*, 2 α-CH Glu(OMe)[18], Ala[4]); 3.99–3.95 (*m*, 1 H of α-CH_2 Gly[11], 2 α-CH Dab(Tfa)[9], Glu(OMe)[7], 1 H of δ-CH_2 Pro[2]); 3.92–3.89 (*m*, 1 H of δ-CH_2 Pro[14]); 3.77–3.76 (*m*, 1 H of α-CH_2 Gly[11], α-CH Val[15], 1 H of δ-CH_2 Pro[14]); 3.67–3.66 (*m*, CH_2OH Phol, 2 Glu(O*Me*)); 3.63 (*s*, Glu(O*Me*)); 3.53–3.47 (*m*, 1 H of δ-CH_2 Pro[2], γ-CH_2 Dab(Tfa)[9]); 2.98–2.94 (*dd*, 1 H of β-CH_2 Phol); 2.77–2.69 (*m*, 1 H of β-CH_2Phol, 1 H of γ-CH_2 Glu(OMe)[7,18,19]); 2.65–2.63 (*m*, 1 H of γ-CH_2(OMe)[18]); 2.53–2.50 (*m*, 1 H of γ-CH_2(OMe)[7,19]); 2.37–2.27 (*m*, 7 H, 1 β-CH Pro[2], Pro[14], Val[15], Glu(OMe)[7,18,19], Dab(Tfa)[9]); 2.21–2.15 (*m*, 3 H, 1 β-CH Glu(OMe)[7,18], Dab(Tfa)[9]); 2.10 (*m*, 2 H, 1 H of γ-CH_2 Pro[2], Pro[14]); 2.08 (*s*, Ac); 2.05–2.04 (*m*, 3 H, 1 H of β-CH_2 Glu(OMe)[19], 1 H of γ-CH_2 Pro[2], Pro[14]); 1.92 (*m*, γ-CH, 1 H of β-CH_2 Leu[12]); 1.84–1.79 (*m*, 2 H, 1 H of β-CH_2 Pro[2], Pro[14]); 1.64–1.49 (*m*, 55 H, 16 Me of 8 Aib, 2 Me of 2 Ala, 1 H of β-CH_2, Leu[12]), 1.09–1.08 (*d*, 1 γ-Me, Val[15]); 0.98–0.92 (*m*, 1 γ-Me of Val[15], 2 δ-Me of Leu[12]). ^{13}C-NMR (150 MHz, $CDCl_3$): 186.55; 179.03; 177.60 (C=O, Gly[11]); 177.10 (C=O, Aib); 177.00; 176.90 (C=O, Aib); 176.30 (C=O, Aib); 175.90 (2 C=O, Ala[4], Glu(OMe)[18]); 175.00 (C=O, Pro[14]) 174.40 (2 C=O, Leu[12], Pro[2]); 174.25 (C=O, Aib); 173.9 (C=O, Val[15]); 173.6 (C=O, Aib[13]); 173.1 (C=O, Glu(OMe)[19]); 172.38; 171.30 (C=O, Ac); 138.53 (C(1), Phol); 129.18 (C(4), Phol); 127.78 (C(2), Phol); 125.78 (C(3), Phol); 118.61; 107.00; 106.91; 91.39; 64.39 ($^{\alpha}$C, Pro[2]); 63.13 ($^{\alpha}$C, Pro[14]); 62.83 ($^{\alpha}$C, Val[15]); 56.85 ($^{\alpha}$C, Aib[13]); 56.75; 56.62 ($^{\alpha}$C, Glu(OMe)[7]); 56.48 ($^{\alpha}$C, Aib[17]); 56.36; 56.23 ($^{\alpha}$C, Aib[5]); 56.17; 56.10 ($^{\alpha}$C, Aib[3]); 55.69 ($^{\alpha}$C, Glu(OMe)[18]); 54.42 ($^{\alpha}$C, Glu(OMe)[19]); 53.14 ($^{\alpha}$C, Phol); 52.23 ($^{\alpha}$C, Leu[12]); 50.56 ($^{\beta}$CH_2OH Phol); 49.22 (1 $^{\delta}$C, Pro[14]); 48.86 (1 $^{\delta}$C, Pro[2]); 43.55 ($^{\alpha}$C, Gly[11]); 43.06; 40.16 ($^{\beta}$C, Leu[12]); 36.76 (1 $^{\beta}$C, Phol); 36.42 ($^{\beta}$C, Dab(Tfa)[9]); 35.63; 30.18 ($^{\beta}$C, Glu(OMe)[7,19]); 29.22 ($^{\beta}$C, Val[15]); 29.02 (1 $^{\beta}$C, Glu(OMe)[7]); 28.83 ($^{\gamma}$C, Pro[14]); 28.48 ($^{\gamma}$C, Pro[2]); 28.02 ($^{\gamma}$C, Dab(Tfa)[9]); 26.11 (1 $^{\beta}$C, Aib); 26.08 (2 $^{\beta}$C, Aib); 25.78 (1 $^{\beta}$C, Aib); 25.73 (1 $^{\beta}$C, Aib); 25.73 (1 $^{\beta}$C, Aib); 25.46 (1 $^{\beta}$C, Aib); 25.41 (1 $^{\beta}$C, Aib); 25.35 (1 $^{\beta}$C, Aib); 25.31 (1 $^{\beta}$C, Aib); 22.51 (2 $^{\beta}$C, Aib); 22.14 (1 $^{\beta}$C, Aib); 22.00 (2 $^{\beta}$C, Aib); 21.87 (1 $^{\beta}$C, Aib); 21.83 (1 $^{\beta}$C, Aib); 21.75 (1 $^{\beta}$C of Aib, 1 $^{\beta}$C of Ala[4]); 21.71 (1 $^{\beta}$C, Ala[6]); 21.02 ($^{\alpha}$C, Ac); 20.04 (1 $^{\delta}$C, Leu[12]); 18.96 (1 $^{\gamma}$C, Val[15]); 18.10 (1 $^{\gamma}$C, Val[15]). ESI-TOF-MS: 2105.50 ($[M+H]^+$; calc. 2105.11); 1053.10 ($[M+2\,H]^{2+}$).

Ac-Aib-Pro-Aib-Ala-Aib-Ala-Glu(OMe)-Aib-Val-Aib-Gly-Leu-Aib-Pro-Val-Aib-Aib-Glu(OMe)-Dab(Tfa)-Phol (**DabTfa19Alm′**; **4**). Yield: 40%. HPLC: t_R 23.48 min (flow rate, 1 ml/min; gradient, 40–90% *B* in 30 min; *C_4 Vydac* column). IR (film on KBr): 3320, 1724, 1658, 1534. ^{1}H-NMR (600 MHz, $CDCl_3$): 8.06–8.04 (*t*, 1 H); 7.99–7.92 (*m*, 7 H); 7.82–7.80 (*m*, 4 H); 7.64–7.41 (*m*, 9 H); 7.30–7.29 (*m*, 3 H); 7.23–7.21 (*m*, 3 H); 7.17–7.16 (*m*, 2 H); 4.49–4.34 (*m*, 2 H); 4.31–4.28 (*m*, 1 H); 4.23–4.20 (*m*, 3 H); 4.05–3.96 (*m*, 6 H); 3.90–3.87 (*m*, 2 H); 3.81–3.806 (*m*, 1 H); 3.75–3.72 (*m*, 3 H); 3.67–3.65 (*m*, 3 H); 3.635 (*s*, 3 H); 3.363 (*s*, 3 H); 3.57–3.49 (*m*, 3 H); 3.42–3.39 (*m*, 2 H); 3.27–3.24 (*m*, 1 H); 2.98–2.81 (*m*, 2 H); 2.71–2.64 (*m*, 2 H); 2.85–2.52 (*m*, 2 H); 2.43–2.17 (*m*, 14 H); 2.10–2.07 (*m*, 6 H); 1.98–1.91 (*m*, 10 H); 1.61–1.44 (*m*, 81 H); 1.30–1.12 (*d*, 3 H); 1.08–1.07 (*d*, 3 H); 1.01–1.00 (*d*, 3 H); 0.95–0.92 (*m*, 9 H). ^{13}C-NMR (150 MHz, $CDCl_3$): 191.26; 189.92; 186.20; 182.09; 182.00; 181.86; 181.79; 176.01; 175.30; 174.14; 173.98; 173.91; 173.71; 173.47; 173.41; 173.30; 173.05; 173.01; 170.63; 147.37; 144.55; 144.04; 138.83; 138.51; 136.12; 135.19; 134.16; 129.64; 128.15; 128.10; 126.18; 106.25; 82.49; 73.69; 73.62; 64.63; 63.55; 56.77; 56.70; 56.57; 56.46; 53.08; 52.85; 51.57; 49.44; 49.40; 49.21; 48.69; 47.65; 46.40; 45.86; 45.29; 33.07; 30.76; 29.99; 29.89; 27.18; 26.97; 26.47; 26.30; 25.50; 23.35; 23.09; 22.74; 22.61; 22.54; 21.23; 19.29; 18.95; 16.80; 16.59. ESI-TOF-MS: 2061.30 ($[M+H]^+$; calc. 2061.12); 1031.12 ($[M+2\,H]^{2+}$).

X-Ray Diffraction Analysis. Colorless crystals of *Ac-Aib-Pro-Aib-Ala-Aib-OBn* (**5**), *Z-Aib-Dab(Tfa)-Aib-Gly-Leu-Aib-O^{t}Bu* (**6**), and *Boc-(Aib)$_2$-Glu(OMe)-Dab(Tfa)-Phol(Bn)* (**7**) were grown by slow evaporation from CH_2Cl_2, a MeOH/Et_2O mixture, and an ^{i}PrOH/MeOH mixture, resp. Data collection was performed on a *Philips PW1100* four-circle diffractometer in the θ–2θ scan mode using graphite-monochromated CuK_α radiation. The structures were solved by direct methods of the SIR 2002 program [99], and refined by full-matrix block least-squares procedures on F^2, using all data, by application of the SHELXL 97 program [100], with anisotropic displacement parameters for all non-H-

atoms, and allowing the positional parameters and the anisotropic displacement parameters to refine at alternate cycles. Evaluation and modelling of disordered parts were performed by exploitation of three-dimensional difference electron-density maps available through the SHELXLe program [101]. Ph Rings, whenever occurring (Phol side chain, Z and Bn protecting groups), were constrained to the idealized geometry. All H-atoms were calculated at idealized positions and refined using a riding model.

The asymmetric unit of **5** is composed of one peptide molecule and one co-crystallized CH_2Cl_2 molecule. Two independent peptide molecules characterize the asymmetric unit of **6**. The Dab side chain in molecule **6B** (*Fig. 7*) is disordered. Its C^{γ} and N^{δ} atoms, and the C=O O-atom of the Tfa protecting group as well, were refined on two sets of positions, each with a population parameter of 0.50. In each of the two independent molecules, the rotationally disorder CF_3 moiety of the Tfa group was refined on two sets of positions, each with a population parameter of 0.50. Restraints were applied to the bond distances and bond angles involving atoms of the disordered parts, as well as to their anisotropic displacement parameters, the latter to approach an isotropic behavior. In **7**, the CF_3 moiety of the Tfa group showed rotational disorder. It was refined on two sets of positions, with population parameters of 0.60 and 0.40, resp. Restraints were applied to the bond distances and bond angles involving atoms of the disordered parts.

Relevant crystallographic data and structure refinement parameters are avaiable as *Supporting Material*. CCDC-942778–942780 contain the crystallographic data for this article. These data can be obtained from *The Cambridge Crystallographic Data Centre via* www.ccdc.cam.ac.uk/data_request/cif.

Antimicrobial Activity Assays. Peptide antibacterial activities were tested against *Gram*-positive and *Gram*-negative bacteria by the standardized disk-diffusion method of *Bauer et al.* [102] according to the National Committee for Clinical Laboratory Standards (NCCLS)-recommended *Mueller–Hilton* agar culture medium (pH 7.2–7.4) [103] and 5-mm diameter paper disks (*Macherey-Nagel 615*, Germany). Disks were prepared by using blank paper disks previously autoclaved and saturated with the peptide soln. The peptide samples were dissolved in DMSO such as to give a 10 mg/ml soln. The peptide-impregnated disks were placed aseptically onto inoculated plates and incubated at 37°. The results were collected after 24 h incubation by measuring the inhibition zones (in mm). The antifungal activity was tested against *Candida albicans* (ATCC 1028, where ATCC stands for *American Type Culture Collection*) strain grown on the *Sabouraud* dextrose agar culture medium [104]. The antibacterial activities were assayed against the reference bacterial strains and clinical isolates (*cf. Table 4*).

REFERENCES

[1] R. M. Epand, R. F. Epand, *J. Pept. Sci.* **2011**, *17*, 298.
[2] H. Duclohier, *Curr. Pharm. Des.* **2010**, *16*, 3212.
[3] R. E. W. Hancock, H.-G. Sahl, *Nat. Biotechnol.* **2006**, *24*, 1551.
[4] H. Brückner, C. Toniolo, *Chem. Biodiversity* **2013**, *10*, 731.
[5] P. A. Pinzon-Arango, R. Nagarajan, T. A. Camesano, *J. Phys. Chem. B* **2013**, *117*, 6364.
[6] M. De Zotti, W. De Borggraave, B. Kaptein, Q. B. Broxterman, S. B. Singh, P. J. Felock, D. J. Hazuda, F. Formaggio, C. Toniolo, *Biopolymers* **2011**, *96*, 49.
[7] C. Peggion, F. Formaggio, M. Crisma, R. F. Epand, R. M. Epand, C. Toniolo, *J. Pept. Sci.* **2003**, *9*, 679.
[8] M. De Zotti, B. Biondi, F. Formaggio, C. Toniolo, L. Stella, Y. Park, K.-S. Hahm, *J. Pept. Sci.* **2009**, *15*, 615.
[9] G. R. Marshall, in 'Intra-Science Chemistry Reports', Ed. N. Kharasch, Gordon and Breach, New York, 1971, p. 305.
[10] I. L. Karle, P. Balaram, *Biochemistry* **1990**, *29*, 6747.
[11] V. Pavone, E. Benedetti, B. Di Blasio, C. Pedone, A. Santini, A. Bavoso, C. Toniolo, M. Crisma, L. Sartore, *J. Biomol. Struct. Dyn.* **1990**, *7*, 1321.
[12] E. Benedetti, B. Di Blasio, V. Pavone, C. Pedone, C. Toniolo, M. Crisma, *Biopolymers* **1992**, *32*, 453.
[13] C. Toniolo, M. Crisma, F. Formaggio, C. Peggion, *Biopolymers* **2001**, *60*, 396.

[14] R. Gessmann, H. Brückner, K. Petratos, *J. Pept. Sci.* **2003**, *9*, 753.
[15] H. Brückner, M. Currle, in 'Second Forum on Peptides', Eds. A. Aubry, M. Marraud, B. Vitoux, Libbey, London, 1989, p. 251.
[16] F. Formaggio, Q. B. Broxterman, C. Toniolo, in 'Houben-Weyl: Methods of Organic Chemistry, Synthesis of Peptides and Peptidomimetics', Eds. M. Goodman, A. Felix, L. Moroder, C. Toniolo, Thieme, Stuttgart, 2003, Vol. E22c, p. 292.
[17] M. De Zotti, B. Biondi, C. Peggion, Y. Park, K.-S. Hahm, F. Formaggio, C. Toniolo, *J. Pept. Sci.* **2011**, *17*, 585.
[18] R. Nagaraj, P. Balaram, *Acc. Chem. Res.* **1981**, *14*, 356.
[19] M. S. P. Sansom, *Prog. Biophys. Mol. Biol.* **1991**, *55*, 139.
[20] R. O. Fox, F. M. Richards, *Nature (London)* **1982**, *300*, 325.
[21] G. A. Woolley, B. A. Wallace, *Biochemistry* **1993**, *32*, 9819.
[22] J. K. Chugh, B. A. Wallace, *Biochem. Soc. Trans.* **2001**, *29*, 565.
[23] G. A. Woolley, *Chem. Biodiversity* **2007**, *4*, 1323.
[24] S. Futaki, K. Asami, *Chem. Biodiversity* **2007**, *4*, 1313.
[25] B. Leitgeb, A. Szekeres, L. Manczinger, C. Vagvölgyi, L. Kredics, *Chem. Biodiversity* **2007**, *4*, 1027.
[26] L. Kredics, A. Szekeres, D. Czifra, C. Vagvölgyi, B. Leitgeb, *Chem. Biodiversity* **2013**, *10*, 744.
[27] N. Stoppacher, N. K. N. Neumann, L. Burgstaller, S. Zeiliger, T. Degenkolb, H. Brückner, R. Schuhmaker, *Chem. Biodiversity* **2013**, *10*, 734.
[28] M. Bortolus, M. De Zotti, F. Formaggio, A. L. Maniero, *Biochim. Biophys. Acta* **2013**, *1828*, 2620.
[29] C. Peggion, I. Coin, C. Toniolo, *Biopolymers* **2004**, *76*, 485.
[30] C. Peggion, M. Jost, C. Baldini, F. Formaggio, C. Toniolo, *Chem. Biodiversity* **2007**, *4*, 1183.
[31] C. Peggion, M. Jost, W. M. De Borggraeve, M. Crisma, F. Formaggio, C. Toniolo, *Chem. Biodiversity* **2007**, *4*, 1256.
[32] R. A. Jose, M. De Zotti, C. Peggion, F. Formaggio, C. Toniolo, W. M. De Borggraeve, *J. Pept. Sci.* **2011**, *17*, 377.
[33] R. Bartucci, R. Guzzi, M. De Zotti, C. Toniolo, L. Sportelli, D. Marsh, *Biophys. J.* **2008**, *94*, 2698.
[34] A. D. Milov, R. I. Samoilova, Y. D. Tsvetkov, M. De Zotti, C. Toniolo, J. Raap, *J. Phys. Chem. B* **2008**, *112*, 13469.
[35] S. Bobone, D. Roversi, L. Giordano, M. De Zotti, F. Formaggio, C. Toniolo, Y. Park, L. Stella, *Biochemistry* **2012**, *51*, 10124.
[36] A. D. Milov, R. I. Samoilova, Y. D. Tsvetkov, M. De Zotti, F. Formaggio, C. Toniolo, J.-W. Handgraaf, J. Raap, *Biophys. J.* **2009**, *96*, 3197.
[37] E. S. Salnikov, M. De Zotti, F. Formaggio, X. Li, C. Toniolo, J. D. J. O'Neil, J. Raap, S. A. Dzuba, B. Bechinger, *J. Phys. Chem. B* **2009**, *113*, 3034.
[38] M. Crisma, C. Peggion, C. Baldini, E. J. MacLean, N. Vedovato, G. Rispoli, C. Toniolo, *Angew. Chem., Int. Ed.* **2007**, *46*, 2047.
[39] A. D. Milov, R. I. Samoilova, Y. D. Tsvetkov, F. Formaggio, C. Toniolo, J. Raap, *J. Am. Chem. Soc.* **2007**, *129*, 9260.
[40] L. Thøgersen, B. Schiøtt, T. Vosegaard, N. C. Nielsen, E. Tajkhorshid, *Biophys. J.* **2008**, *95*, 4337.
[41] A. D. Milov, M. I. Samoilova, Y. D. Tsvetkov, M. Jost, C. Peggion, F. Formaggio, M. Crisma, C. Toniolo, J.-W. Handgraaf, J. Raap, *Chem. Biodiversity* **2007**, *4*, 1275.
[42] D. Marsh, M. Jost, C. Peggion, C. Toniolo, *Chem. Biodiversity* **2007**, *4*, 1269.
[43] L. Stella, M. Burattini, C. Mazzuca, A. Palleschi, M. Venanzi, I. Coin, C. Peggion, C. Toniolo, B. Pispisa, *Chem. Biodiversity* **2007**, *4*, 1299.
[44] E. R. de Azevedo, W. G. Hu, T. J. Bonagamba, K. Schmidt-Rohr, *J. Chem. Phys.* **2000**, *112*, 8988.
[45] W. Luo, M. Hong, *J. Am. Chem. Soc.* **2006**, *128*, 7242.
[46] E. S. Salnikov, J. Raya, C. Peggion, G. Ballano, M. De Zotti, C. Toniolo, J. Raap, B. Bechinger, **2014**, submitted.
[47] C. U. Hjørringgaard, J. M. Pedersen, T. Vosegaard, N. C. Nielsen, T. Skrydstrup, *J. Org. Chem.* **2009**, *74*, 1329.
[48] M. Gobbo, C. Poloni, M. De Zotti, C. Peggion, B. Biondi, G. Ballano, F. Formaggio, C. Toniolo, *Chem. Biol. Drug. Des.* **2010**, *75*, 169.

[49] S. Stamm, H. Heimgartner, *Eur. J. Org. Chem.* **2004**, 3820.
[50] S. Stamm, A. Linden, H. Heimgartner, *Helv. Chim. Acta* **2006**, *89*, 1.
[51] S. Stamm, H. Heimgartner, *Tetrahedron* **2006**, *62*, 9671.
[52] M. Jost, J.-C. Greie, N. Stammer, S. D. Wilking, K. Altendorf, N. Sewald, *Angew. Chem., Int. Ed.* **2002**, *41*, 4267.
[53] M. Jost, S. Weigelt, T. Huber, Z. Majer, J.-C. Greie, K. Altendorf, N. Sewald, *Chem. Biodiversity* **2007**, *4*, 1170.
[54] S. Weigelt, T. Huber, F. Hofmann, M. Jost, M. Ritzefeld, B. Luy, C. Freudenberger, Z. Majer, E. Vass, J.-C. Greie, L. Panella, B. Kaptein, Q. B. Broxterman, H. Kessler, K. Altendorf, M. Hollosi, N. Sewald, *Chem. – Eur. J.* **2012**, *18*, 478.
[55] A. D. Konar, E. Vass, M. Hollosi, Z. Majer, G. Grüber, K. Frese, N. Sewald, *Chem. Biodiversity* **2013**, *10*, 942.
[56] H. Wenschuh, M. Beyermann, H. Haber, J. K. Seydel, E. Krause, M. Bienert, L. A. Carpino, A. El-Faham, F. Albericio, *J. Org. Chem.* **1995**, *60*, 405.
[57] E. Salnikov, J. Raya, C. Peggion, G. Ballano, C. Toniolo, J. Raap, B. Bechinger, in 'Peptides: Building Bridges. Proc. 22nd American Peptide Symposium', Ed. M. Lebl, Prompt Sci. Publ., San Diego, CA, 2011, p. 118.
[58] R. Nagaraj, P. Balaram, *Tetrahedron* **1981**, *37*, 1263.
[59] H. Schmitt, G. Jung, *Liebigs Ann. Chem.* **1985**, 321.
[60] P. Wipf, H. Heimgartner, *Helv. Chim. Acta* **1990**, *73*, 13.
[61] U. Slomczynska, J. Zabrocki, K. Kaczmarek, M. T. Leplawy, D. D. Beusen, G. R. Marshall, *Biopolymers* **1992**, *32*, 1461.
[62] K. Akaji, Y. Tamai, Y. Kiso, *Tetrahedron* **1997**, *53*, 567.
[63] P. K. Mandal, J. S. McMurray, *J. Org. Chem.* **2007**, *72*, 6599.
[64] L. J. Bellamy, 'The Infrared Spectra of Complex Molecules', 2nd edn., Methuen, London, 1966.
[65] M. T. Cung, M. Marraud, J. Néel, *Ann. Chim. (Paris)* **1972**, *7*, 183.
[66] D. F. Kennedy, M. Crisma, C. Toniolo, D. Chapman, *Biochemistry* **1991**, *30*, 6541.
[67] M. Goodman, C. Toniolo, *Biopolymers* **1968**, *6*, 1673.
[68] S. Beychok, in 'Poly-α-Amino Acids: Protein Models for Conformational Studies', Ed. G. D. Fasman, Dekker, New York, 1967, p. 293.
[69] M. C. Manning, R. W. Woody, *Biopolymers* **1991**, *31*, 569.
[70] C. Toniolo, A. Polese, F. Formaggio, M. Crisma, J. Kamphuis, *J. Am. Chem. Soc.* **1996**, *118*, 2744.
[71] F. Formaggio, M. Crisma, P. Rossi, P. Scrimin, B. Kaptein, Q. B. Broxterman, J. Kamphuis, C. Toniolo, *Chem. – Eur. J.* **2006**, *6*, 4498.
[72] C. Toniolo, E. Benedetti, *Trends Biochem. Sci.* **1991**, *16*, 350.
[73] K. A. Bolin, G. L. Millhauser, *Acc. Chem. Res.* **1991**, *32*, 1027.
[74] G. L. Millhauser, *Biochemistry* **1995**, *34*, 3873.
[75] K. Wüthrich, 'NMR of Proteins and Nucleic Acids', Wiley, New York, 1986.
[76] A. Bax, M. F. Summers, *J. Am. Chem. Soc.* **1986**, *108*, 2093.
[77] E. Benedetti, C. Pedone, C. Toniolo, G. Némethy, M. S. Pottle, H. A. Scheraga, *Int. J. Pept. Protein Res.* **1980**, *16*, 156.
[78] E. Benedetti, C. Pedone, C. Toniolo, M. Dudek, G. Némethy, H. A. Scheraga, *Int. J. Pept. Protein Res.* **1983**, *21*, 163.
[79] E. Benedetti, in 'Chemistry and Biodiversity of Amino Acids, Peptides and Proteins', Ed. B. Weinstein, Dekker, New York, 1982, Vol. 6, p. 105.
[80] T. Ashida, Y. Tsunogae, I. Tanaka, T. Yamane, *Acta Crystallogr., Sect. B* **1987**, *43*, 212.
[81] W. B. Schweizer, J. D. Dunitz, *Helv. Chim. Acta* **1982**, *65*, 1547.
[82] Y. Paterson, S. M. Rumsey, E. Benedetti, G. Némethy, H. A. Scheraga, *J. Am. Chem. Soc.* **1981**, *103*, 2947.
[83] G. Valle, M. Crisma, F. Formaggio, C. Toniolo, G. Jung, *Liebigs Ann. Chem.* **1987**, 1055.
[84] C. Ramakrishnan, N. Prasad, *Int. J. Protein Res.* **1971**, *3*, 209.
[85] R. Taylor, O. Kennard, W. Versichel, *Acta Crystallogr., Sect. B* **1984**, *40*, 280.
[86] C. H. Görbitz, *Acta Crystallogr., Sect. B* **1989**, *45*, 390.

[87] C. M. Venkatachalam, *Biopolymers* **1968**, *6*, 1425.
[88] C. Toniolo, *CRC Crit. Rev. Biochem.* **1980**, *9*, 1.
[89] G. D. Rose, L. M. Gierasch, J. A. Smith, *Adv. Protein Chem.* **1985**, *37*, 1.
[90] V. Pavone, G. Gaeta, A. Lombardi, F. Nastri, O. Maglio, C. Isernia, M. Saviano, *Biopolymers* **1996**, *38*, 705.
[91] C. Toniolo, G. M. Bonora, A. Bavoso, E. Benedetti, B. Di Blasio, V. Pavone, C. Pedone, *Biopolymers* **1983**, *22*, 205.
[92] T. Ashida, M. Kakudo, *Bull. Chem. Soc. Jpn.* **1974**, *47*, 1129.
[93] E. Benedetti, A. Bavoso, B. Di Blasio, V. Pavone, C. Pedone, C. Toniolo, G. M. Bonora, *Biopolymers* **1983**, *22*, 305.
[94] D. Cremer, J. A. Pople, *J. Am. Chem. Soc.* **1975**, *97*, 1354.
[95] E. S. Salnikov, H. Friedrich, X. Li, P. Bertani, S. Reissmann, C. Hertweck, J. D. J. O'Neil, J. Raap, B. Bechinger, *Biophys. J.* **2009**, *96*, 86.
[96] L. A. Carpino, *J. Am. Chem. Soc.* **1993**, *115*, 4397.
[97] A. Bax, D. G. Davis, *J. Magn. Reson.* **1985**, *65*, 355.
[98] C. Griesinger, G. Otting, K. Wüthrich, R. R. Ernst, *J. Am. Chem. Soc.* **1988**, *110*, 7870.
[99] M. C. Burla, M. Camalli, B. Carrozzini, G. L. Cascarano, C. Giacovazzo, G. Polidori, R. Spagna, *J. Appl. Crystallogr.* **2003**, *36*, 1103.
[100] G. M. Sheldrick, *Acta Crystallogr., Sect. A* **2008**, *64*, 112.
[101] C. B. Hübschle, G. M. Sheldrick, B. Dittrich, *J. Appl. Crystallogr.* **2011**, *44*, 1281.
[102] A. W. Bauer, W. M. Kirby, J. C. Sherris, M. Turck, *Am. J. Clin. Pathol.* **1966**, *45*, 493.
[103] National Committee for Clinical Laboratories Standards, Wayne, PA, 1997 (publication N. M2-A6).
[104] National Committee for Clinical Laboratory Standards, Villanova, PA, 1992. Reference Method for Broth Dilution Antifungal Susceptibility Testing for Yeasts: Proposed Standard M.27.P. NCCLS.

Received December 17, 2013